Arch. Mech., 42, 3, pp. 347–375, Warszawa 1990

Theoretical and computational aspects of large plastic deformations involving strain-induced anisotropy and developing voids (*)

R. LAMMERING (GÖTTINGEN), R. B. PĘCHERSKI (WARSZAWA) and E. STEIN (HANNOVER)

THE AIM OF THE PAPER is to formulate the constitutive equations of elastic-plastic solids with strain-induced anisotropy and growing voids and to develop numerical algorithms to solve the equations proposed. The anisotropic hardening of porous material is described in terms of the combined isotropic-kinematic hardening model which appears to be a combination of the hardening laws of Prager and Ziegler. The considerations are limited to the associated flow rule, what is related with the simplified assumption that the nucleation of voids during the process is neglected. The rate equations are formulated by means of substructure corotational rates involving the relation for plastic spin. The theory derived is complemented with finite element formulation and numerical examples. In the numerical approach the operator-split and return mapping strategy is applied. The Newton–Raphson algorithm is used to solve the system of nonlinear equations. For this purpose the Lagrangian form of the principle of virtual work is linearized. The finite element implementation is based on the convected coordinate formulation. The problems of simple shear and the necking of a cylindrical bar were computed to show the correctness of the numerical procedure and to describe the behaviour of the material subjected to large plastic deformations and developing voids.

Celem pracy jest sformułowanie równań konstytutywnych ciał sprężysto-plastycznych z indukowaną odkształceniem plastycznym anizotropią i rozwijającymi się pustkami oraz zbudowanie odpowiednich algorytmów numerycznych rozwiązujących te równania. Wzmocnienie anizotropowe materiału porowatego jest opisane za pomocą modelu wzmocnienia izotropowo-kinematycznego, który jest pewną kombinacją modeli Pragera i Zieglera. Rozważania ograniczono do stowarzyszonego prawa płynięcia, co jest związane z upraszczającym założeniem o zaniedbaniu efektu nukleacji pustek w czasie procesu. Równania prędkościowe zostały sformułowane z zastosowaniem prędkości współobrotowych ze strukturą materiału, co pociąga za sobą zastosowanie równania na spin plastyczny. Teorię uzupełniono sformułowaniem algorytmu dla metody elementów skończonych i przykładami numerycznymi. Zastosowano przy tym strategię dekompozycji operatora sprężysto-plastycznego i metodę rzutowania powrotnego. Do rozwiązania układu równań nieliniowych wykorzystano metodę Newtona–Raphsona. Zlinearyzowano w tym celu Lagranżowską formę zasady prac przygotowanych. Implementacja metody elementów skończonych opiera się na sformułowaniu równań we współrzędnych konwekcyjnych. Rozwiązane numerycznie problemy prostego ścinania i szyjkowania cylindrycznego pręta wykazują poprawność procedury numerycznej oraz opisują zachowanie się materiału przy dużych odkształceniach plastycznych i rozwijających się pustkach.

Целью работы является формулировка определяющих уравнений упруго-пластических тел с индуцированной, пластической деформацией, анизотропией и развивающимися пустотами, а также построение соответствующих численных алгоритмов решающих эти уравнения. Анизотропное упрочнение пористого материала описано при помощи модели изотропно-кинематического упрочнения, которая является некоторой комбинацией моделей Прагера и Зиглера. Рассуждения ограничены ассоциированным законом течения, что связано с упрощающим предположением о пренебрежении эффектами нуклеации пустот во время процесса. Скоростные уравнения сформулированы с применением совращательных скоростей со структурой материала, что приводит с собой применение уравнения для пластического спина. Теория пополнена формулировкой алго-

(*) The main results of this paper were presented during the 4th Bilateral Symposium PRL-BRD on Mechanics of Inelastic Solids and Structures, 13–19 September, 1987 in Kraków-Mogilany.

ритма для метода конечных элементов и численными примерами. При этом применена стратегия декомпозиции упруго-пластического оператора и метод обратной проекции. Для решения системы нелинейных уравнений использован метод Ньютона–Рафсона. С этой целью линеаризована лагранжевая форма принципа виртуальных работ. Имплементация метода конечных элементов опирается на формулировке уравнений в конвекционных координатах. Решенные численно проблемы простого сдвига и образование шейки цилиндрического стержня показывают правильность численной процедуры, а также описывают поведение материала при больших пластических деформациях и развивающихся пустотах.

1. Introduction

MODELLING of ductile fracture, metal forming and related strain localization produces an increasing demand for the adequate constitutive description of the inelastic behaviour of engineering materials and efficient numerical strategies. The constitutive equations for small elastic and finite plastic deformations with strain-induced anisotropy modelled as combined isotropic-kinematic hardening have been implemented in finite element programs (cf. e.g., HUGHES [1]). A constitutive description of plastic deformations taking into account nucleation and growth of voids was studied by GURSON [2, 3] and NEEDLEMAN and RICE [4]. Further references can be found in the review given by TVERGAARD [5]. On the other hand, it has been found by TVERGAARD [6] and HUTCHINSON and TVERGAARD [7] that the application of kinematic hardening provides a more realistic prediction of the strain at the onset of localization than the plasticity with isotropic hardening. In MEAR and HUTCHINSON [8] and TVERGAARD [5, 9] the Ziegler model of kinematic hardening with the *Zaremba–Jaumann* rate was applied for the numerical analysis of the effect of yield surface curvature on localization in porous plastic solids described by means of the modified Gurson model [2, 3]. The effect of strain-induced anisotropy in plastic flow and localization of damaged solids was also studied by DUSZEK and PERZYNA [10].

The introduction of tensorial internal variables, e.g., the kinematic hardening parameter (back stress), is related to the formulation of objective rate-type constitutive equations. The application of the Zaremba–Jaumann rate can lead to the non-adequate prediction of the material reaction while the finite shearing with pertinent large rotations of the principal axes of the back stress tensor plays the dominant role. A detailed discussion of this problem with pertinent references is provided in PAULUN and PĘCHERSKI [11, 12] and in PĘCHERSKI [13].

In the computational approach to the solution of large plastic deformation problems the incremental methods of initial stress or tangent matrix have been widely implemented (cf. e.g. ZIENKIEWICZ [14] and and NEEDLEMAN and TVERGAARD [15] or KLEIBER [16]). Although these techniques appear very successful in many applications, they create certain difficulties for some classes of problems, particularly when advanced plastic flow is involved. The method of initial stresses uses the same coefficient stiffness matrix for all iterations and gives unconditional but very slow convergence. In tangent stiffness methods divergence may occur. The tangent stiffness methods are implicit, with coefficient matrix updates based on the instantaneous plastic state. Very small increments are necessary in such a case to provide the required accuracy. This involves high computation costs.

Numerous ways of improving these schemes have been proposed using either extensions or mixtures of both methods, or approximating to the tangent stiffness matrix to avoid the expensive reinversion required at every iteration (cf. HELLEN [17]).

An important aspect in computational plasticity is to retain the consistency condition which requires that the stress trajectory be confined to the elastic domain, what is difficult to inforce exactly. Frequently, projection techniques have been introduced to restore consistency. The search for an efficient method leads to the application of a "return mapping" algorithm (cf. PINSKY, ORTIZ and TAYLOR [18] and HUGHES [1]). This technique consists in solving for every time step an incremental linear elastic problem (elastic predictor) followed by the application of a return mapping algorithm to the stresses to restore the consistency condition (plastic corrector). Such a procedure appears to have been suggested first by WILKINS [19] and thoroughly analysed by KRIEG and KRIEG [20] and SCHREYER, KULAK and KRAMER [21], largely restricted to perfect plasticity with the Huber–Mises yield condition. The extension of the radial return method to accommodate linear isotropic and kinematic hardening was provided by KRIEG and KEY [22]. In the case of the general convex yield surface, the closest point algorithms have been formulated (cf. ORTIZ [23], ORTIZ *et al.* [24] and PLANK and STEIN [25]). As it was pointed out by ORTIZ and SIMO [26] the application of the closest point procedure to non-trivial plasticity models requires calculation of the gradients of the plastic flow direction, the normal to the yield surface, the plastic moduli and the elasticity tensor. In order to avoid the laborious evaluation of such quantites, ORTIZ and SIMO [26, 27] proposed a new class of return mapping algorithms applicable to a general class of plastic and viscoplastic constitutive models. The algorithm is formulated solely on the basis of the yield function, the normal to the yield surface, the direction of plastic flow and the tangent elastic moduli without involving their gradients. In this procedure the elastic predictor stress is returned to the yield surface in successive steps. Each one of these steps involves a projection of the stresses onto a linear approximation of the yield surface or "cut".

The extension of the return mapping algorithms to nonlinear hardening rules and the development of the consistent tangent moduli was considered by SIMO and TAYLOR [28] The consistent linearization of the response function resulting from the integration algorithm provides the quadratic rate of asymptotic convergence. When the radial return algorithms are employed in conjunction with the so-called elasto-plastic tangent moduli that are obtained from the continuum model by enforcement of the consistency condition, the quadratic rate of convergence is lost. This fact was recognized by NAGTEGAAL [29] for a plastic material with isotropic hardening. The problem of linearization of the discretized weak form of the momentum balance equation (virtual work) and the consistency between the tangent operator and the integration algorithm employed in the solution of the incremental problem were considered by HUGHES and PISTER [30] and PINSKY *et al.* [18] as well as by WRIGGERS [31] and GRUTTMANN and STEIN [32].

It has been emphasized by PINSKY *et al.* [18] that some numerical integration schemes applied in the past to spatial rate constitutive equations have employed difference operations on the spatial stress components. However, such quantities have no mathematical sense, for the linear space operations can only be applied to relate tensor fields which are determined on the common configuration. The set of all configurations of a body

can be shown to be a smooth manifold (cf. MARSDEN and HUGHES [33]). A tensor field defined on a particular configuration is a member of the tangent space associated with that configuration. Therefore, tensor fields defined on different configurations belong to different linear spaces and cannot be combined by means of the linear space operations such as addition and subtraction. This leads to the concept of pulling back of spatial quantities to a common reference configuration in order to define precisely difference operators to be used in numerical algorithms. This is the reason why the linearization of tensor fields defined on the spatial configuration can be properly expressed in terms of pull back, push forward and Lie derivative (cf. Appendix for the pertinent definitions and references). These geometrical concepts are applied sometimes for the formulation of the covariant theory. Covariance embodies material frame indifference with respect to arbitrary spatial diffeomorphisms. In [33] the mathematical theory of elasticity was formulated as a covariant theory. Some attempts have also been made to extend such an approach to inelastic materials with internal variables (cf. e.g. SIMO [34] and PERZYNA [35]). The first comprehensive and critical analysis of the application of the Lie-derivative in continuum mechanics was provided by GUO ZHONG-HENG [36]. This problem is also tackled in the paper.

The aim of the paper is to formulate the new constitutive equations of elastic-plastic solids with strain-induced anisotropy and developing voids. The model proposed by GURSON [2, 3] and generalized by MEAR and HUTCHINSON [8] is extended to formulate the flow condition and the equation describing the growth of voids. The anisotropic hardening of porous material is described in terms of the combined isotropic-kinematic hardening model which appears to be a certain combination of the hardening laws of Prager and Ziegler. The considerations are limited to the associated flow rule; this is related to the simplified assumption that the nucleation of voids during the process is neglected. The new rate equations are formulated by means of the objective rates involving the relation for plastic spin.

The theory derived is complemented with finite element formulation and numerical examples. In the numerical approach, the discussed operator split and return mapping strategy is applied. The Newton–Raphson algorithm is used to solve the system of nonlinear equations. The Lagrangian form of the principle of virtual work is linearized for this purpose. Finite element implementation is based on a Lagrangian convective coordinate formulation as described by GREEN and ZERNA [37] (cf. NEEDLEMAN [38]). Due to this the total Lagrangian formulation of the principle of virtual work can be directly related to the spatial rate equations, for the components of the Kirchhoff stress tensor are equal to the components of the second Piola-Kirchhoff stress tensor and the components of the rate of deformation tensor, referred to the current configuration, are equal to the components of the material rate of the Green–Lagrange strain tensor, referred to the initial configuration. By the integration of the rate constitutive equations of hypoelasticity and elastoplasticity formulated in the current configuration, the principle of objectivity was preserved (cf. PINSKY *et al.* [39]). Geometrically, the calculation of the elastoplastic case can be understood as the return mapping of the point in the stress space, reached in the elastic predictor step, onto the yield surface in successive steps. At every step, the updated stresses are computed by projecting the result of the previous

iteration onto the linear approximation of the yield function. The finite element formulation is implemented into the general purpose computer program FEAP (Finite Element Analysis Program), developed by R. L. Taylor and described in ZIENKIEWICZ [14]. Two examples are considered to show the correctness of the numerical procedure and to describe the behaviour of the material: the problem of simple shear and the necking of a cylindrical bar (cf. LAMMERING (40)].

2. Kinematics

Consider the motion φ_t of a body described by introducing the initial configuration B at time t_0 and the current configuration $\varphi(B)$ at time t. The position vectors $\mathbf{X}$ and $\mathbf{x}$ represent a particle X in the configurations B and $\varphi(B)$, respectively; $\mathbf{x} = \varphi_t(\mathbf{X})$. A convective coordinate net is introduced, which can be visualized as being inscribed on the body in the initial configuration and deforming with the material. The convected coordinates, $\Theta^i (i = 1, 2, 3)$ serve as particle labels and the position vectors $\mathbf{X}$ and $\mathbf{x}$ are considered as functions of Θ^i and the time t, i.e.,

$$\begin{aligned} \mathbf{X} &= \hat{\mathbf{X}}(\Theta^i, t), \\ \mathbf{x} &= \hat{\mathbf{x}}(\Theta^i, t). \end{aligned} \tag{2.1}$$

Covariant base vectors of the material net in the intial configuration, $\mathbf{G}_i$, and in the current configuration, $\mathbf{g}_i$, are defined by the total differential

$$\begin{aligned} d\mathbf{X} &= \frac{\partial \hat{\mathbf{X}}}{\partial \Theta^i} d\Theta^i = \mathbf{G}_i d\Theta^i, \quad i = 1, 2, 3, \\ d\mathbf{x} &= \frac{\partial \hat{\mathbf{x}}}{\partial \Theta^i} d\Theta^i = \mathbf{g}_i d\Theta^i, \quad i = 1, 2, 3. \end{aligned} \tag{2.2}$$

Contravariant base vectors are related to the covariant base vectors by the equations

$$\begin{aligned} \mathbf{G}_i \cdot \mathbf{G}^j &= \delta_i^j, \quad i, j = 1, 2, 3, \\ \mathbf{g}_i \cdot \mathbf{g}^j &= \delta_i^j, \quad i, j = 1, 2, 3. \end{aligned} \tag{2.3}$$

Application of the chain rule lead to the following relation between the base vectors:

$$\mathbf{g}_i = \frac{\partial \hat{\mathbf{x}}}{\partial \mathbf{X}} \cdot \frac{\partial \mathbf{X}}{\partial \Theta^i} = \mathbf{F} \cdot \mathbf{G}_i, \tag{2.4}$$

where $\mathbf{F}$ is the deformation gradient. The tensor $\mathbf{F}$ can be presented in the following form:

$$\mathbf{F} = \mathbf{g}_i \otimes \mathbf{G}^i = \delta_j^i (\mathbf{g}_i \otimes \mathbf{G}^j) = g_{ij} (\mathbf{g}^i \otimes \mathbf{G}^j) = G^{ij} (\mathbf{g}_i \otimes \mathbf{G}_j), \tag{2.5}$$

where

$$\begin{aligned} g_{ij} &= \mathbf{g}_i \cdot \mathbf{g}_j \\ G^{ij} &= \mathbf{G}^i \cdot \mathbf{G}^j. \end{aligned} \tag{2.6}$$

The *Green–Lagrange strain* tensor $\mathbf{E}$ is given by

$$\mathbf{E} = \frac{1}{2} (\mathbf{F}^T \cdot \mathbf{F} - \mathbf{1}), \tag{2.7}$$

or due to Eq. (2.5)

$$\mathbf{E} = \frac{1}{2}(g_{ij} - G_{ij})\mathbf{G}^i \otimes \mathbf{G}^j. \tag{2.8}$$

The material time derivative of $\mathbf{E}$ is given by the expression

$$\dot{\mathbf{E}} = \frac{1}{2}(\dot{\mathbf{F}}^T \cdot \mathbf{F} + \mathbf{F}^T \cdot \dot{\mathbf{F}}) \cdot \mathbf{G}_j. \tag{2.9}$$

where the dot indicates the material time derivative. The component form of Eq. (2.9) reads

$$\dot{E}_{ij} = \mathbf{G}_i \cdot \dot{\mathbf{E}} \cdot \mathbf{G}_j = \frac{1}{2}\mathbf{G}_i \cdot (\dot{\mathbf{F}}^T \cdot \mathbf{F} + \mathbf{F}^T \cdot \dot{\mathbf{F}}) \cdot \mathbf{G}_j. \tag{2.10}$$

The *Almansi* strain tensor $\mathbf{e}$ is referred to the current configuration and may be expressed in the form

$$\mathbf{e} = \frac{1}{2}(\mathbf{1} - \mathbf{F}^{-T} \cdot \mathbf{F}^{-1}) \tag{2.11}$$

or due to Eq. (2.5)

$$\mathbf{e} = \frac{1}{2}(g_{ij} - G_{ij})\mathbf{g}^i \otimes \mathbf{g}^j. \tag{2.12}$$

The velocity gradient grad $\mathbf{v}$ leads to the following kinematical relations:

$$\begin{aligned} &\mathbf{L} = \operatorname{grad}\mathbf{v} = \dot{\mathbf{F}} \cdot \mathbf{F}^{-1}, \\ &\mathbf{L} = \mathbf{D} + \mathbf{W}, \\ &\mathbf{D} = \frac{1}{2}(\mathbf{L} + \mathbf{L}^T), \quad \mathbf{W} = \frac{1}{2}(\mathbf{L} - \mathbf{L}^T), \end{aligned} \tag{2.13}$$

where $\mathbf{D}$ is the rate of deformation tensor and $\mathbf{W}$ is the material spin tensor.

The components of $\mathbf{D}$ with respect to the covariant base vector of the current configuration are calculated as

$$D_{ij} = \mathbf{g}_i \cdot \mathbf{D} \cdot \mathbf{g}_j = \frac{1}{2}\mathbf{g}_i \cdot (\dot{\mathbf{F}} \cdot \mathbf{F}^{-1} + \mathbf{F}^{-1} \cdot \dot{\mathbf{F}}^T) \cdot \mathbf{g}_j = \frac{1}{2}\mathbf{G}_i \cdot (\dot{\mathbf{F}}^T \cdot \mathbf{F} + \mathbf{F}^T \cdot \dot{\mathbf{F}}) \cdot \mathbf{G}_j. \tag{2.14}$$

Comparison with Eq. (2.10) shows that the components of the material derivative of the *Green–Lagrange* strain tensor, referred to the initial configuration and those of the rate of deformation tensor, referred to the current configuration, are the same.

The application of the *Lie* derivative to the *Almansi* strain tensor $\mathbf{e}$ yields

$$L_v\mathbf{e} = \mathbf{D}. \tag{2.15}$$

In plasticity of single crystals it is usually assumed that the dislocations traversing a volume element produce a change of its shape but they do not change its lattice orientation. The macroscopic counterpart of such a situation in finite deformation plasticity of polycrystals is the *Mandel's* concept of the intermediate relaxed configuration, called isoclinic, in which the chosen director triad always keeps the same orientation with respect to the fixed axes.

The relaxed configuration is related to the assumption of the existence of the instantaneous natural state (KLEIBER and RANIECKI [41]). Due to this the unique decomposition of the deformation gradient $\mathbf{F}$ is provided, MANDEL [42], LORET [43], KLEIBER and RANIECKI [41] and SIDOROFF and TEODOSIU [44]

$$\mathbf{F} = \mathbf{F}_{el} \cdot \mathbf{F}_{pl}, \tag{2.16}$$

where $\mathbf{F}_{el}$ and $\mathbf{F}_{pl}$ correspond to elastic and plastic transformations, respectively (cf. also DAFALIAS [45], PĘCHERSKI [13] and RANIECKI and SAMANTA [46] for a more detailed discussion of these concepts and further references).

The following decomposition can be derived (cf. SIMO and ORTIZ [27] and WRIGGERS and STEIN [47]):

$$L_v \mathbf{e} = L_v \mathbf{e}_{el} + L_v \mathbf{e}_{pl}, \tag{2.17}$$

where

$$\begin{aligned} \mathbf{e}_{el} &= \frac{1}{2}(\mathbf{1} - \mathbf{F}_{el}^{-T} \cdot \mathbf{F}_{el}^{-1}), \\ \mathbf{e}_{pl} &= \frac{1}{2}(\mathbf{F}_{el}^{-T} \cdot \mathbf{F}_{el}^{-1} - \mathbf{F}^{-T} \cdot \mathbf{F}^{-1}) \end{aligned} \tag{2.18}$$

are respectively the elastic and plastic *Almansi* strain tensors. The formula (2.17) is valid in case of large elastic and large plastic deformations. If the elastic deformations are assumed to be small, it can be rewritten as

$$\mathbf{D} = \mathbf{D}_{el} + \mathbf{D}_{pl}, \tag{2.19}$$

where

$$\mathbf{D}_{el} = \frac{1}{2}(\mathbf{L}_{el} + \mathbf{L}_{el}^T), \quad \mathbf{D}_{pl} = \frac{1}{2}(\mathbf{L}_{pl} + \mathbf{L}_{pl}^T), \tag{2.20}$$

$$\mathbf{L}_{el} = \dot{\mathbf{F}}_{el} \cdot \mathbf{F}_{el}^{-1}, \quad \mathbf{L}_{pl} = \dot{\mathbf{F}}_{pl} \cdot \mathbf{F}_{pl}^{-1}. \tag{2.21}$$

3. Balance laws

The axiom of local mass conservation reads

$$\varrho_0 = \det \mathbf{F} \varrho, \tag{3.1}$$

where ϱ is the density. The relation between the volume element in the initial configuration dV and the current configuration dv is given by

$$dv = \frac{\varrho_0}{\varrho} dV = \det \mathbf{F} dV. \tag{3.2}$$

The principle of balance of local momentum is expressed by

$$\mathrm{Div} \mathbf{P} + \varrho_0 \mathbf{b} = \varrho_0 \ddot{\mathbf{x}}, \tag{3.3}$$

where $\mathbf{P}$ denotes the 1st *Piola–Kirchhoff* stress tensor. The body force $\varrho_0 \mathbf{b}$ and the inertial force $\varrho_0 \mathbf{x}$ will be neglected in the following.

The principle of local moment of momentum takes the form

$$\mathbf{P}\cdot\mathbf{F}^T = \mathbf{F}\cdot\mathbf{P}^T \tag{3.4}$$

and shows, that $\mathbf{P}$ is not symmetric. The relations for the tensors of the 1st *Piola–Kirchhoff* stress $\mathbf{P}$, the 2nd *Piola–Kirchhoff* stress $\mathbf{S}$ and the *Cauchy* stress $\mathbf{T}$ as well as the *Kirchhoff* stress $\boldsymbol{\tau}$ are given as follows:

$$\mathbf{S} = \mathbf{F}^{-1}\cdot\mathbf{P}, \tag{3.5}$$

$$\mathbf{T} = \frac{1}{\det\mathbf{F}}\mathbf{P}\cdot\mathbf{F}^T, \tag{3.6}$$

$$\boldsymbol{\tau} = (\det\mathbf{F})\mathbf{T} = \mathbf{F}\cdot\mathbf{S}\cdot\mathbf{F}^T. \tag{3.7}$$

In the convective coordinates the components of the 2nd *Piola–Kirchhoff* stress tensor $\mathbf{S} = S^{ij}\mathbf{G}_i\otimes\mathbf{G}_j$ and the components of the *Kirchhoff* stress tensor $\boldsymbol{\tau} = \tau^{ij}_{\ \ j}\mathbf{g}_i\otimes\mathbf{g}_j$ are given by the identity

$$\tau^{ij} = S^{ij}. \tag{3.8}$$

This can be shown in the same way as the identity $E_{ij} = D_{ij}$ in Eqs. (2.10) and (2.14).

In the equations describing the behaviour of elastic-plastic deformations with combined isotropic-kinematic hardening, the rates of stress and back stress appear. The formalism of the Lie derivative is sometimes applied to define objective stress fluxes.

According to the discussion in the appendix, the representation of the Lie derivative of the stress tensor field is not unique. The expression of the *Kirchhoff* stress $\boldsymbol{\tau}$ respectively in the covariant, contravariant and both mixed bases

$$\begin{aligned}\boldsymbol{\tau}_1 &= \tau^{ij}\mathbf{g}_i\otimes\mathbf{g}_j,\\ \boldsymbol{\tau}_2 &= \tau_{ij}\mathbf{g}^i\otimes\mathbf{g}^j,\\ \boldsymbol{\tau}_3 &= \tau^i_{\ j}\mathbf{g}_i\otimes\mathbf{g}^j,\\ \boldsymbol{\tau}_4 &= \tau^j_{\ i}\mathbf{g}^i\otimes\mathbf{g}_j\end{aligned} \tag{3.9}$$

can lead to four different representations of the Lie derivative $L_v\boldsymbol{\tau}$ (MARSDEN and HUGHES [33], pp. 99–102, box 6.1). The Lie derivative of the *Kirchhoff* stress tensor $\boldsymbol{\tau}$ expressed in the covariant base vectors takes in the absolute notation the form

$$L_v\boldsymbol{\tau}_1 = \dot{\boldsymbol{\tau}}_1 - \mathbf{L}\cdot\boldsymbol{\tau}_1 - \boldsymbol{\tau}_1\cdot\mathbf{L}^T. \tag{3.10}$$

This representation corresponds to the *Oldroyd* derivative. Equivalently, the *Truesdell* derivative of the *Cauchy* stress $\boldsymbol{\sigma}_1 = \sigma^{ij}\mathbf{g}_i\otimes\mathbf{g}_j$ can be written as follows:

$$L_v\boldsymbol{\sigma}_1 = L_v\boldsymbol{\tau}_1 + \boldsymbol{\tau}_1\,\mathrm{tr}\mathbf{D}. \tag{3.11}$$

All the representations discussed above are reduced to the one unique expression

$$L_v\boldsymbol{\tau} \equiv \overset{\nabla}{\boldsymbol{\tau}} = \dot{\boldsymbol{\tau}} + \boldsymbol{\tau}\cdot\mathbf{W} - \mathbf{W}\cdot\boldsymbol{\tau}, \tag{3.12}$$

if and only if the velocity field $\mathbf{v}$ is a *Killing* vector field for the metric $\mathbf{g}$. In such a case, each map $\varphi_{t,s}$ of the flow of $\mathbf{v}$ is an isometry and $\mathbf{D} = \mathbf{0}$. The rate $\overset{\nabla}{\boldsymbol{\tau}}$ corresponds to the *Zaremba–Jaumann* derivative of the stress tensor $\boldsymbol{\tau}$.

When $\mathbf{D} \neq \mathbf{0}$, the relation between the *Zaremba–Jaumann* rate and the representation of $L_v\boldsymbol{\tau}$ in the covariant basis (*Oldroyd* rate) takes the form

$$\overset{\nabla}{\boldsymbol{\tau}} = L_v\boldsymbol{\tau} + \boldsymbol{\tau}\cdot\mathbf{D} + \mathbf{D}\cdot\boldsymbol{\tau}. \tag{3.13}$$

This relation will be used frequently in further considerations, therefore the index "1" will be omitted in the following.

The first comprehensive and critical discussion of the application of the Lie derivative in continuum mechanics was presented by GUO ZHONG-HENG [36] where also physical conditions were considered. One of these conditions, very important in the theory of plasticity, was formulated by PRAGER [48]. It requires that vanishing of the objective time derivative of the second order tensor $\mathbf{A}$ should induce vanishing of the time derivative of its arbitrary invariant:

$$L_v\mathbf{A} = \mathbf{0} \rightarrow \dot{\mathrm{I}}_{\mathrm{A}} = \dot{\mathrm{II}}_{\mathrm{A}} = \dot{\mathrm{III}}_{\mathrm{A}} = 0. \tag{3.14}$$

Fulfilment of this condition leads to the *Zaremba–Jumann*-type representation of the objective rate of $\mathbf{A}$.

The principle of virtual work is a formulation which is equivalent to the balance of momentum, Eq. (3.3). This work principle, often referred to as weak form of the balance of momentum, is applicable in a general way because no further assumptions, e.g., the existence of a potential, are made.

The derivation of the principle of virtual work starts with the balance of momentum, Eq. (3.3), which is scalar multiplied with a vector-valued function $\boldsymbol{\eta}$, usually called virtual displacement or test function. The integration over the volume B of the body under consideration yields

$$\int_B \varrho_0 \mathbf{b}\cdot\boldsymbol{\eta}\,dV + \int_B \mathrm{Div}\mathbf{P}\cdot\boldsymbol{\eta}\,dV = 0. \tag{3.15}$$

The boundary conditions are introduced for the displacement field $\mathbf{u}$ and the surface tractions $\mathbf{t}$ on the part ∂B_u and the part on ∂B_σ of the surface of the body, respectively

$$\begin{aligned} \bar{\mathbf{u}} &= \mathbf{u} \qquad \text{on} \quad \partial B_u, \\ \bar{\mathbf{t}} &= \mathbf{P}\cdot\mathbf{n}_0 \quad \text{on} \quad \partial B_\sigma. \end{aligned} \tag{3.16}$$

The partial integration of the second term of Eq. (3.15) using the divergence theorem gives with the boundary conditions (3.16)

$$G(\mathbf{u},\boldsymbol{\eta}) = \int_B [\mathbf{P}:\mathrm{Grad}\boldsymbol{\eta} - \varrho_0\mathbf{b}\cdot\boldsymbol{\eta}]dV - \int_{\partial B_\sigma} \bar{\mathbf{t}}\cdot\boldsymbol{\eta}\,dA = 0. \tag{3.17}$$

Introducing the 2nd *Piola–Kirchhoff* stress tensor, Eq. (3.5), the principle of virtual work may be rewritten as

$$G(\mathbf{u},\boldsymbol{\eta}) = \int_B [\mathbf{S}:\delta\mathbf{E} - \varrho_0\mathbf{b}\cdot\boldsymbol{\eta}]dV - \int_{\partial B_\sigma} \bar{\mathbf{t}}\cdot\boldsymbol{\eta}\,dA = 0. \tag{3.18}$$

4. Constitutive equations

4.1. Constitutive relations of elasticity

For the sake of brevity and simplicity the isothermal processes will be considered only. Assume the mechanical state variables $(\hat{\mathbf{S}}, \hat{\mathbf{a}})$ corresponding to the instantaneous natural state in the intermediate configuration, where

$$\hat{\mathbf{S}} = \mathbf{F}_{el}^{-1} \cdot \boldsymbol{\tau} \cdot \mathbf{F}_{el}^{-T} \tag{4.1}$$

and $\hat{\mathbf{a}}$ represent the structural variables, e.g., the back stress $\hat{\boldsymbol{\alpha}}$ and the isotropic hardening parameter $\hat{\varkappa}$.

The elastic *Green–Lagrange* strain $\mathbf{E}_{el} = \frac{1}{2}(\mathbf{F}_{el}^{T}\mathbf{F}_{el} \cdot -\mathbf{1})$ can be calculated from the free enthalpy $\mathscr{H}$ per unit mass that can be assumed in the form (MANDEL [42] and KLEIBER and RANIECKI [41])

$$\mathscr{H} = \mathscr{H}(\hat{\mathbf{S}}, \hat{\mathbf{a}}) = \mathscr{H}_1(\hat{\mathbf{S}}) + \mathscr{H}_2(\hat{\mathbf{a}}), \tag{4.2}$$

$$\mathbf{E}_{el} = -\hat{\varrho}\frac{\partial \mathscr{H}}{\partial \hat{\mathbf{S}}}. \tag{4.3}$$

The rate of elastic strain is given by

$$\dot{\mathbf{E}}_{el} = \hat{\mathsf{N}} : \dot{\hat{\mathbf{S}}}, \tag{4.4}$$

where

$$\hat{\mathsf{N}} = -\hat{\varrho}\frac{\partial^2 \mathscr{H}}{\partial \hat{\mathbf{S}} \partial \hat{\mathbf{S}}} \tag{4.5}$$

is the elastic compliance tensor and $\hat{\varrho}$ is the density related with the relaxed configuration. The transformation of Eqs. (4.1) and (4.4) to the current configuration yields

$$\mathbf{D}_{el} = \mathsf{N} : \overset{\circ}{\boldsymbol{\tau}}, \tag{4.6}$$

where

$$N_{ijkl} = (\det \mathbf{F}_{el})(F_{el}^{-1})_{\alpha i}(F_{el}^{-1})_{\beta j}(F_{el}^{-1})_{\gamma k}(F_{el}^{-1})_{\delta l}\hat{N}_{\alpha\beta\gamma\delta} \tag{4.7}$$

and

$$\overset{\circ}{\boldsymbol{\tau}} = \dot{\boldsymbol{\tau}} - \mathbf{L}_{el} \cdot \boldsymbol{\tau} - \boldsymbol{\tau} \cdot \mathbf{L}_{el}^{T}. \tag{4.8}$$

This is the *Oldroyd* rate with respect to the elastic transformation $\mathbf{E}_{el}$. Taking into account the decomposition

$$\mathbf{L}_{el} = \mathbf{D}_{el} + \mathbf{W}_{el}, \tag{4.9}$$

Eq. (4.8) reads

$$\overset{\circ}{\boldsymbol{\tau}} = \dot{\boldsymbol{\tau}} - \mathbf{W}_{el} \cdot \boldsymbol{\tau} + \boldsymbol{\tau} \cdot \mathbf{W}_{el} - \mathbf{D}_{el} \cdot \boldsymbol{\tau} - \boldsymbol{\tau} \cdot \mathbf{D}_{el}, \tag{4.10}$$

where $\mathbf{W}_{el}$ is the elastic spin and $\mathbf{D}_{el}$ is the elastic rate of deformation.

It is typical for most deformed metallic solids that their distortional elastic strains remain small under arbitrary loading conditions, whereas they can undergo large elastic dilatational changes in shape under very high pressure. RANIECKI and NGUYEN [49] have shown, studying thermomechanics of isotropic elastic-plastic solids at finite strain and arbitrary pressure, that the tensor of elastic moduli in *Eulerian* description can be expressed in terms of derivations of the free energy as simply as in the case of infinitesimal strains, provided the logarithmic elastic strain is adopted as a state variable and that the values of the ratios of principal elastic stretches $\mathbf{U}_{el}$, $\mathbf{F}_{el} = \mathbf{R}_{el} \cdot \mathbf{U}_{el}$, are limited in a certain interval (cf. RANIECKI and NGUYEN [49] for further details). The large elastic dilatational changes will be neglected in our further considerations. The dilatation produced by progressively developing voids will be discussed instead. It is therefore justified to assume that $\mathbf{U}_{el}$ is close to unity. In such a case Eq. 4.10 can be approximated by the *Zaremba–Jaumann* rate with respect to $\mathbf{W}_{el}$

$$\check{\boldsymbol{\tau}} \approx \mathring{\boldsymbol{\tau}} = \dot{\boldsymbol{\tau}} - \mathbf{W}_{el} \cdot \boldsymbol{\tau} + \boldsymbol{\tau} \cdot \mathbf{W}_{el} \tag{4.11}$$

and the relation of elasticity can be rewritten in the form

$$\mathring{\boldsymbol{\tau}} = \mathsf{C} : \mathbf{D}_{el}, \quad \mathsf{C} = \mathsf{N}^{-1} \tag{4.12}$$

where C can be specified as follows:

$$\mathsf{C} = \lambda(\mathbf{1} \otimes \mathbf{1}) + 2\mu\mathbf{I}. \tag{4.13}$$

Let us observe that due to the decomposition

$$\mathbf{W} = \mathbf{W}_{el} + \mathbf{W}_{pl} \tag{4.14}$$

Eq. (4.11) can be expressed by means of the material spin $\mathbf{W}$ and the plastic spin $\mathbf{W}_{pl}$

$$\mathring{\boldsymbol{\tau}} = \dot{\boldsymbol{\tau}} - (\mathbf{W} - \mathbf{W}_{pl}) \cdot \boldsymbol{\tau} + \boldsymbol{\tau} \cdot (\mathbf{W} - \mathbf{W}_{pl}) = \overset{\nabla}{\boldsymbol{\tau}} + \mathbf{W}_{pl} \cdot \boldsymbol{\tau} - \boldsymbol{\tau} \cdot \mathbf{W}_{pl} \tag{4.15}$$

and an additional equation for plastic spin is required. The rate expressed as in Eq. (4.15) is sometimes interpreted as the rate corotational with the substructure (cf. PĘCHERSKI [13]). This rate fulfills the discussed *Prager* condition and therefore will be applied in the formulation of the constitutive equations of plasticity.

4.2. The model of porous plastic solid

For porous (dilatant) ductile materials, GURSON [2], [3] proposed an approximate yield criterion and a flow rule that take into account the influence of hydrostatic stress on plastic deformation and void growth. The yield criterion is based on an upper bound solution for spherically symmetric deformations of a rigid plastic material obeying the *Huber-Mises* yield criterion around a single spherical void. The initial yield surface is given by

$$\Phi_0 = \frac{3}{2} \frac{\boldsymbol{\tau}' : \boldsymbol{\tau}'}{\sigma_y^2} + 2f \cosh\left(\frac{\operatorname{tr}\boldsymbol{\tau}}{2\sigma_y}\right) - (1 + f_0) = 0. \tag{4.16}$$

Here, $\boldsymbol{\tau}'$ denotes the deviator of the *Kirchhoff* stress tensor, f_0 the initial void volume fraction and σ_y the initial yield stress of the matrix material.

In order to study the influence of the yield surface curvature on flow localization in dilatant plasticity, MEAR and HUTCHINSON [8] take into account the combined isotropic-kinematic hardening. In this case, the radius of the yield surface σ_M is calculated by

$$\sigma_M = (1-b)\sigma_y + b_e. \tag{4.17}$$

The constant b, $b \in [0, 1]$, influences the way the material hardens: $b = 1$ corresponds to kinematic, $b = 0$ to isotropic hardening. The yield stress in case of purely isotropic hardening is denoted by σ_e. Introducing the back stress tensor $\boldsymbol{\alpha}$ the flow surface of the material takes the form

$$\Phi = \frac{3}{2}\frac{(\boldsymbol{\tau}'-\boldsymbol{\alpha}):(\boldsymbol{\tau}'-\boldsymbol{\alpha})}{\sigma_M^2} + 2f\cosh\left(\frac{\operatorname{tr}(\boldsymbol{\tau}-\boldsymbol{\alpha})}{2\sigma_M}\right) - (1+f^2) = 0. \tag{4.18}$$

For $f = 0$ the yield conditions (4.16) and (4.18) reduce to the *Huber–Mises* criterion. It is assumed by BISHOP, HILL [50] as well as by BERG [51] and GURSON [2, 3], that the direction of plastic flow is normal to the yield surface of the porous material if the matrix material obeys the *Huber-Mises* yield criterion

$$\mathbf{D}_{\mathrm{pl}} = \frac{1}{H}(\boldsymbol{\mu}:\mathring{\boldsymbol{\tau}})\frac{\partial \Phi}{\partial \boldsymbol{\tau}} = \dot{\Lambda}\frac{\partial \Phi}{\partial \boldsymbol{\tau}}. \tag{4.19}$$

The vector $\boldsymbol{\mu}$ is perpendicular to the yield surface and H is a scalar function. The changes of the yield stress and the void volume fraction are calculated by

$$\dot{\sigma}_M = b\dot{\sigma}_e = b\zeta\frac{(\boldsymbol{\tau}-\boldsymbol{\alpha}):\mathbf{D}_{\mathrm{pl}}}{(1-f)\sigma_M}, \tag{4.20}$$

$$\dot{f} = (1-f)\operatorname{tr}\mathbf{D}_{\mathrm{pl}}. \tag{4.21}$$

Due to Eqs. (4.17) and (4.18) different values of b produce a family of combined isotropic-kinematic hardening surfaces. Following MEAR and HUTCHINSON [8] it is assumed that each member of the family is constructed such that under proportional stressing it coincides with *Gurson's* purely isotropic hardening version. The difference between any two members of the family appears only when departures from proportional loading path occur. This requirement formulated by

$$\frac{\boldsymbol{\tau}-\boldsymbol{\alpha}}{\sigma_M} = \frac{\boldsymbol{\tau}}{\sigma_e} \tag{4.22}$$

is fulfilled when the back stress tensor $\boldsymbol{\alpha}$ is evaluated by Eq. (4.22)

$$\mathring{\boldsymbol{\alpha}} = \hat{R}(\boldsymbol{\tau}, \boldsymbol{\alpha})(\boldsymbol{\tau}-\boldsymbol{\alpha}), \tag{4.23}$$

where $\mathring{\boldsymbol{\alpha}}$ is defined in the same way as $\mathring{\boldsymbol{\tau}}$ in Eq. (4.15). Specifying the evolution function $\hat{R}(\boldsymbol{\tau}, \boldsymbol{\alpha})$ the different hardening laws can be obtained. For example, taking

$$\hat{R}(\boldsymbol{\tau}, \boldsymbol{\alpha}) = Q(\boldsymbol{\tau}-\boldsymbol{\alpha}):\frac{\partial \Phi}{\partial \boldsymbol{\tau}}, \tag{4.24}$$

the *Ziegler* hardening law proposed by MEAR and HUTHINSON [8] is obtained. The function Q could be evaluated from Eq. (4.22) and the consistency condition

$$\dot{\Phi} = \frac{\partial \Phi}{\partial \boldsymbol{\tau}} : \mathring{\boldsymbol{\tau}} + \frac{\partial \Phi}{\partial \boldsymbol{\alpha}} : \mathring{\boldsymbol{\alpha}} + \frac{\partial \Phi}{\partial \sigma_M} \dot{\sigma}_M + \frac{\partial \Phi}{\partial f} \dot{f} = 0. \tag{4.25}$$

This is not suitable for the radial return and the predictor-corrector procedure implemented here, for in the calculation of the plastic corrector step, cf. Eq. (5.19) and (5.20), the consistency condition is applied and all increments of $\boldsymbol{\tau}$, $\boldsymbol{\alpha}$, σ_M, and f should be expressed in terms of $\dot{\Lambda}$. Using the hardening law (4.24) would be related to the double application of Eq. (4.25) what leads to tautology. It is more convenient from the numerical point of view to assume that the rate of back stress $\boldsymbol{\alpha}$ is linearly dependent on $\mathbf{D}_{\mathrm{pl}}$. Such a dependence is provided by the *Prager* hardening law

$$\mathring{\boldsymbol{\alpha}}^{\mathrm{Pr}} = c\mathbf{D}^{\mathrm{pl}}. \tag{4.26}$$

When $f = 0$ the parameter $c = \frac{2}{3}\xi$. In porous materials, however, c should be determined from an additional condition. The condition (4.22) will be assumed here. Consider the projection of $\mathring{\boldsymbol{\alpha}}^{\mathrm{Pr}}$ in the direction of $(\boldsymbol{\tau}-\boldsymbol{\alpha})$:

$$\mathring{\boldsymbol{\alpha}} = \tilde{c} \frac{\mathbf{D}_{\mathrm{pl}} : (\boldsymbol{\tau}-\boldsymbol{\alpha})}{\sqrt{(\boldsymbol{\tau}-\boldsymbol{\alpha}) : (\boldsymbol{\tau}-\boldsymbol{\alpha})}} (\boldsymbol{\tau}-\boldsymbol{\alpha}). \tag{4.27}$$

Taking into account Eqs. (4.19) and (4.27) the evolution equation (4.23) can be rewritten as

$$\mathring{\boldsymbol{\alpha}} = \dot{\Lambda} R(\boldsymbol{\tau}-\boldsymbol{\alpha}), \tag{4.28}$$

where R will be determined from Eqs. (4.22) and (4.25).

The function H is calculated from the consistency condition (4.25) and the evolution equations (4.20), (4.21) and (4.28) as well as (4.22)

$$H = \frac{\xi}{(1-f)\sigma_M^2} \left[\frac{\partial \Phi}{\partial \boldsymbol{\tau}} : (\boldsymbol{\tau}-\boldsymbol{\alpha}) \right]^2 - (1-f) \frac{\sigma_e}{\sigma_M} \frac{\partial \Phi}{\partial f} \frac{\partial \Phi}{\partial \boldsymbol{\tau}} : \mathbf{1}. \tag{4.29}$$

The calculation of the vector μ in Eq. (4.19) yields

$$\mu = \frac{\partial \Phi}{\partial \boldsymbol{\tau}}. \tag{4.30}$$

Thus the flow rule (4.19) can be rewritten as

$$\mathbf{D}_{\mathrm{pl}} = \frac{1}{H} \left[\frac{\partial \Phi}{\partial \boldsymbol{\tau}} : \mathring{\boldsymbol{\tau}} \right] \frac{\partial \Phi}{\partial \boldsymbol{\tau}} = \dot{\Lambda} \frac{\partial \Phi}{\partial \boldsymbol{\tau}}. \tag{4.31}$$

This means that an associated flow rule is obtained. The function R is calculated by use of Eqs. (4.22) and (4.25):

$$R = (1-b) \frac{H + \frac{\partial \Phi}{\partial f}(1-f)\mathrm{tr} \frac{\partial \Phi}{\partial \boldsymbol{\tau}} \frac{\sigma_y}{\sigma_M}}{\frac{\partial \Phi}{\partial \boldsymbol{\tau}} : (\boldsymbol{\tau}-\boldsymbol{\alpha})}. \tag{4.32}$$

4.3. Elastic-plastic material

Taking notice of the additive decomposition of the rate of the deformation tensor into an elastic and a plastic part (cf. 2.19), the combination of the constitutive description of an elastic material, (4.12) and plastic material, (4.31), yields the elastic-plastic constitutive relation

$$\mathbf{D} = \left[\mathsf{C}^{-1} + \frac{1}{H}\frac{\partial \Phi}{\partial \boldsymbol{\tau}} \otimes \frac{\partial \Phi}{\partial \boldsymbol{\tau}}\right] : \mathring{\boldsymbol{\tau}}. \tag{4.33}$$

Its inverse formulation is calculated as

$$\mathring{\boldsymbol{\tau}} = \left[\mathsf{C} - \frac{\left(\mathsf{C} : \frac{\partial \Phi}{\partial \boldsymbol{\tau}}\right) \otimes \left(\mathsf{C} : \frac{\partial \Phi}{\partial \boldsymbol{\tau}}\right)}{H + \frac{\partial \Phi}{\partial \boldsymbol{\tau}} : \mathsf{C} : \frac{\partial \Phi}{\partial \boldsymbol{\tau}}}\right] : \mathbf{D}. \tag{4.34}$$

The constitutive equations discussed are complemented by the equation for plastic spin $\mathbf{W}_{\mathrm{pl}}$ proposed by PAULUN and PĘCHERSKI [11] (cf. also PĘCHERSKI [13] for more detail discussion and further references)

$$\mathbf{W}_{\mathrm{pl}} = \eta(\boldsymbol{\alpha} \cdot \mathbf{D} - \mathbf{D} \cdot \boldsymbol{\alpha})_u, \tag{4.35}$$

where

$$(\boldsymbol{\alpha} \cdot \mathbf{D} - \mathbf{D} \cdot \boldsymbol{\alpha})_u = \frac{\boldsymbol{\alpha} \cdot \mathbf{D} - \mathbf{D} \cdot \boldsymbol{\alpha}}{\sqrt{(\boldsymbol{\alpha} \cdot \mathbf{D} - \mathbf{D} \cdot \boldsymbol{\alpha}) : (\boldsymbol{\alpha} \cdot \mathbf{D} - \mathbf{D} \cdot \boldsymbol{\alpha})}} \tag{4.36}$$

and

$$\eta = \sqrt{\frac{3}{2}}\,\frac{3(\varepsilon_{\mathrm{pl}}^{\mathrm{eq}})^2}{1 + 3(\varepsilon_{\mathrm{pl}}^{\mathrm{eq}})^2}\,\dot{\varepsilon}_{\mathrm{pl}}^{\mathrm{eq}}, \tag{4.37}$$

$$\dot{\varepsilon}_{\mathrm{pl}}^{\mathrm{eq}} = \sqrt{\frac{2}{3}\,\mathbf{D}_{\mathrm{pl}} \cdot \mathbf{D}_{\mathrm{pl}}} \tag{4.38}$$

and

$$\varepsilon_{\mathrm{pl}}^{\mathrm{eq}} = \int_0^t \dot{\varepsilon}_{\mathrm{pl}}^{\mathrm{eq}}\, dt. \tag{4.39}$$

The relation for plastic spin (4.36) has been derived from the analysis of the problem of finite simple shear. The function η (4.37) results from the difference between the constant angular speed produced by the material spin $\mathbf{W}$ and the angular velocity of the material line element lying initially perpendicular to the direction of shear. The angular velocity of such a material line embodies the average lattice spin over the polycrystalline volume element. The function specified in Eqs. (4.37) provides satisfactory results in the analysis of the simple shear traction problem and the axial elongation predicted theoretically conforms with experimentally observed *Swift* effect, PAULUN and PĘCHERSKI [12]. The analysis of the simple shear traction problem under reverse loading requires modification of the function (4.37), as discussed in [13].

5. Finite element formulation

The starting point for the finite element formulation is the principle of virtual work, (3.17). Since this equation is nonlinear in the displacements $\mathbf{u}$, an iterative numerical algorithm has to be employed for its solution.

The *Newton–Raphson* algorithm will be implemented to solve the system of nonlinear equations. For this purpose it is necessary to linearize the principle of virtual work.

5.1. The linearization of the principle of virtual work

The basic equation for the linearization procedure with respect to a deformed configuration, described by the displacement vector $\bar{\mathbf{u}}$, is expressed by

$$G(\bar{\mathbf{u}}, \boldsymbol{\eta}; \Delta\mathbf{u}) = G(\bar{\mathbf{u}}, \boldsymbol{\eta}) + DG(\bar{\mathbf{u}}, \boldsymbol{\eta}) \cdot \Delta\mathbf{u}. \tag{5.1}$$

Equation (5.1) may be interpreted as the expansion of Eq. (3.18) into a *Taylor* series. The expression $DG\ (\bar{\mathbf{u}}, \boldsymbol{\eta}) \cdot \Delta\mathbf{u}$, in which $\Delta\mathbf{u}$ denotes the displacement increment, is calculated by the formula

$$DG(\bar{\mathbf{u}}, \boldsymbol{\eta}) \cdot \Delta\mathbf{u} = \frac{d}{d\varepsilon} [G(\bar{\mathbf{u}} + \varepsilon\Delta\mathbf{u}, \boldsymbol{\eta})]|_{0\varepsilon=}. \tag{5.2}$$

The *Newton–Raphson* algorithm is obtained when Eq. (5.1) equals zero

$$G(\bar{\mathbf{u}}, \boldsymbol{\eta}) = -DG(\bar{\mathbf{u}}, \boldsymbol{\eta}) \cdot \Delta\mathbf{u}. \tag{5.3}$$

The linearization of the principle of virtual work (3.18) results in

$$DG(\bar{\mathbf{u}}, \boldsymbol{\eta}) \cdot \Delta\mathbf{u} = \int_{B_0} \{\mathrm{Grad}\,\Delta\mathbf{u} \cdot \bar{\mathbf{S}} + \bar{\mathbf{F}} \cdot [D\mathbf{S}(\bar{\mathbf{u}}) \cdot \Delta\mathbf{u}]\} : \mathrm{Grad}\,\boldsymbol{\eta}\, dV, \tag{5.4}$$

in which quantities with a bar are related to the known configuration. The surface tractions $\bar{\mathbf{t}}$ vanish because they do not depend on the displacements. The linearization of the 2nd *Piola–Kirchhoff* stress tensor is calculated by use of the chain rule

$$D\mathbf{S}(\bar{\mathbf{u}}) \cdot \Delta\mathbf{u} = \frac{\partial \mathbf{S}}{\partial \mathbf{E}} : D\mathbf{E}(\bar{\mathbf{u}}) \cdot \Delta\mathbf{u} = \frac{1}{2} (\bar{\mathbf{F}}^T \cdot \mathrm{Grad}\,\Delta\mathbf{u} + \mathrm{Grad}^T\,\Delta\mathbf{u} \cdot \bar{\mathbf{F}}). \tag{5.5}$$

Now, the tangent operator (5.4) may be rewritten in the form

$$\begin{aligned} DG(\bar{\mathbf{u}}, \boldsymbol{\eta}) \cdot \Delta\mathbf{u} = {} & \int_{B_0} \mathrm{Grad}\,\Delta\mathbf{u} \cdot \bar{\mathbf{S}} : \mathrm{Grad}\,\boldsymbol{\eta}\, dV \\ & + \frac{1}{2} \int_{B_0} \bar{\mathbf{F}} \cdot \left[\frac{\partial \mathbf{S}}{\partial \mathbf{E}} : (\bar{\mathbf{F}}^T \cdot \mathrm{Grad}\,\Delta\mathbf{u} + \mathrm{Grad}^T\,\Delta\mathbf{u} \cdot \bar{\mathbf{F}}) \right] : \mathrm{Grad}\,\boldsymbol{\eta}\, dV. \end{aligned} \tag{5.6}$$

The expression $\partial\mathbf{S}/\partial\mathbf{E}$ depending on the constitutive equation is calculated by its spatial counterpart. Following WRIGGERS [31] the linearization of a spatial tensor field, i.e., the *Kirchhoff* stress tensor $\boldsymbol{\tau}$, is obtained by its *Lie* derivative

$$L_u \boldsymbol{\tau} = \mathbf{F} \cdot \left\{ \frac{d}{d\varepsilon} [\mathbf{F}^{-1} \cdot \boldsymbol{\tau}(\bar{\mathbf{u}} + \varepsilon\Delta\mathbf{u}) \cdot \mathbf{F}^{-T}]_{\varepsilon=0} \right\} \cdot \mathbf{F}^T = \mathbf{F} \cdot \left\{ \frac{d}{d\varepsilon} [\mathbf{S}(\bar{\mathbf{u}} + \varepsilon\Delta\mathbf{u})]_{\varepsilon=0} \right\} \cdot \mathbf{F}^T. \tag{5.7}$$

It is visible that the linearization of the *Kirchhoff* stress tensor $\boldsymbol{\tau}$ is the spatial formulation of the linearized 2nd *Piola–Kirchhoff* stress tensor $\mathbf{S}$. The components of these linearized tensors are equal, c.f. (2.14). By the chain rule it follows

$$L_u(\boldsymbol{\tau}) = \frac{\partial \boldsymbol{\tau}}{\partial \mathbf{e}} : L_u(\mathbf{e}). \tag{5.8}$$

In a convective coordinate net, the components of $L_u(\mathbf{e})$ are equal to the components of the linearized *Green–Lagrange* strain tensor $D\mathbf{E}(\mathbf{u}) \cdot \Delta\mathbf{u}$, c.f. Eq. (5.5). This means that the components of $\partial \mathbf{S}/\partial \mathbf{E}$ can be substituted by the components of $\partial \boldsymbol{\tau}/\partial \mathbf{e}$

$$\frac{\partial S^{ij}}{\partial E_{kl}} = \frac{\partial \tau^{ij}}{\partial e_{kl}}, \tag{5.9}$$

which will be calculated from the constitutive equation.

5.2. Integration of rate constitutive equations

The algorithm is based on updating the known variables at a converged configuration B_n, deformation gradient $\mathbf{F}_n$, plastic variables $\boldsymbol{\alpha}_n$, σ_{Mn}, f_n and stresses $\boldsymbol{\tau}_n$ to their corresponding values $\mathbf{F}_{n+1}$, $\boldsymbol{\alpha}_{n+1}$, σ_{Mn+1}, f_{n+1} and $\boldsymbol{\tau}_{n+1}$ on the updated configuration B_{n+1}. The geometric update from B_n to B_{n+1} is assumed to be given.

From an algorithmic point of view special care must be taken in the integration of rate constitutive equations formulated in the current configuration because the principle of objectivity has to be preserved (PINSKY, ORITZ, PISTER [20]).

In a material description the integration scheme is given by

$$\mathbf{S}_{n+1} = \mathbf{S}_n + \int_{t_n}^{t_{n+1}} \dot{\mathbf{S}}\, dt. \tag{5.10}$$

Introducing Eq. (3.7) and an intermediate configuration given by the deformation gradient $\mathbf{F}_{n+\alpha}$

$$\mathbf{F}_{n+\alpha} = \alpha \mathbf{F}_{n+1} + (1-\alpha)\mathbf{F}_n, \tag{5.11}$$

Eq. (5.10) may be expressed by the *Kirchhoff* stress tensor with

$$\mathbf{F}_{n+1}^{-1} \cdot \boldsymbol{\tau}_{n+1} \cdot \mathbf{F}_{n+1}^{-T} = \mathbf{F}_n^{-1} \cdot \boldsymbol{\tau}_n \cdot \mathbf{F}_n^{-T} + \int_{t_n}^{t_{n+1}} \mathbf{F}_{n+\alpha}^{-1} \cdot \boldsymbol{\tau}_n \cdot \mathbf{F}_{n+\alpha}^{-T}\, dt. \tag{5.12}$$

Objectivity is preserved by the integration algorithm for $\alpha = 0.5$. This means that the increment of stress has to be calculated in an intermediate configuration.

5.2.1. The hypo-elastic case. In order to calculate the components of $\partial \tau^{ij}/\partial e_{kl}$ from Eq. (5.9) the approximation

$$\frac{\partial \tau^{ij}}{\partial e_{kl}} = \frac{\partial L_v(\tau^{ij})}{\partial D_{kl}} \tag{5.13}$$

is made. The constitutive equation (4.12) is rewritten with the help of Eq. (3.13) in the form

$$L_v(\boldsymbol{\tau}) = \mathbf{C}:\mathbf{D} - \boldsymbol{\tau}\cdot\mathbf{D} - \mathbf{D}\cdot\boldsymbol{\tau}. \tag{5.14}$$

The index notation $L_v(\tau^{ij}) = (C^{ijkl} - \tau^{ik}g^{jl} - \tau^{kj}g^{il})D_{kl}$ makes the derivative with respect to D_{kl} easier and leads to

$$\frac{\partial L_v(\tau^{ij})}{\partial D_{kl}} = P^{ijkl} = C^{ijkl} - \tau^{ik}g^{jl} - \tau^{kj}g^{il}. \tag{5.15}$$

These components replacing the components of $\partial\mathbf{S}/\partial\mathbf{E}$ in Eq. (5.6) complete the tangent operator.

Equation (5.12) demands to refer all quantities of Eq. (5.14) to an intermediate configuration. This is done for the elasticity tensor $C^{ijkl} = \mu(g^{ik}g^{jl} + g^{il}g^{jk}) + \lambda g^{ij}g^{kl}$ by calculating the quantities g^{ij} from the deformation gradient $\mathbf{F}_{n+\alpha}$ of this configuration

$$g^{ij}_{n+\alpha} = \mathbf{G}^i \cdot (\mathbf{F}^T_{n+\alpha}\mathbf{F}_{n+\alpha})\cdot\mathbf{G}^j, \tag{5.16}$$

and for the stress tensor $\boldsymbol{\tau}$ by the pull back/push forward operation

$$\boldsymbol{\tau}_{n+\alpha} = \mathbf{F}_{n+\alpha}\cdot(\mathbf{F}_n^{-1}\cdot\boldsymbol{\tau}_n\cdot\mathbf{F}_n^{-T})\cdot\mathbf{F}^T_{n+\alpha}. \tag{5.17}$$

5.2.2. The elastic-plastic case. In consequence of the additive structure of the constitutive equations for elastic-plastic problems, return mapping algorithms have been proposed for the integration of the constitutive equations, splitting the calculation into an elastic and a plastic part with the application of the methodology presented in SIMO, ORTIZ [27] and ORTIZ, SIMO [26].

For the moment it is assumed that the deformation process from the configuration B_n to B_{n+1} is purely elastic and that there is no plastic response of the material. Combining the plastic variables $\boldsymbol{\alpha}$, σ_M, and f into the vector $\mathbf{q}$ the elastic constitutive equations can now be summarized as follows:

$$\begin{aligned} \mathbf{D} &= \mathbf{D}_{\mathrm{el}} + \mathbf{D}_{\mathrm{pl}} = \mathbf{D}(t), \\ L_v(\boldsymbol{\tau}) &= \mathbf{C}:\mathbf{D} - \boldsymbol{\tau}\cdot\mathbf{D} - \mathbf{D}\cdot\boldsymbol{\tau}, \\ \mathbf{D}_{\mathrm{pl}} &= \mathbf{0}, \\ L_v(\mathbf{q}) &= \mathbf{0}. \end{aligned} \tag{5.18}$$

The stresses calculated in this way generally violate the yield condition. Therefore, this elastic predictor step has to be followed by the plastic corrector. The plastic part of the constitutive equations is defined by

$$\begin{aligned} \mathbf{D} &= \mathbf{D}_{\mathrm{el}} + \mathbf{D}_{\mathrm{pl}} = \mathbf{0}, \\ L_v(\boldsymbol{\tau}) &= -\mathbf{C}:\mathbf{D}_{\mathrm{pl}}, \\ \mathbf{D}_{\mathrm{pl}} &= \dot{\Lambda}\frac{\partial \Phi}{\partial \boldsymbol{\tau}}, \\ L_v(\mathbf{q}) &= \dot{\Lambda}\mathbf{h}(\mathbf{q}, \boldsymbol{\tau}). \end{aligned} \tag{5.19}$$

In this equation $\mathbf{h}$ denotes a simplified notation for the evolution equation of the plastic variables, summarizing Eqs. (4.20) (4.21) and (4.28). The right hand sides of Eqs. (5.18) and (5.19) add up to the right hand side of the total rate constitutive equation.

The numerical procedure in calculating the unknown values in the updated configuration is as follows: After the elastic predictor step, which is a straightforward calculation, the stresses violating the yield surface are computed iteratively in the plastic corrector step. For this purpose the yield condition is expanded into a *Taylor* series in order to calculate the unknown parameter $\dot{\Lambda}$.

$$\Phi = \Phi|_{\substack{\tau=\tau_0\\ q=q_0}} + \frac{\partial \Phi}{\partial \boldsymbol{\tau}}\Big|_{\substack{\tau=\tau_0\\ q=q_0}} : \mathring{\boldsymbol{\tau}} + \frac{\partial \Phi}{\partial \boldsymbol{\alpha}}\Big|_{\substack{\tau=\tau_0\\ q=q_0}} : \mathring{\boldsymbol{\alpha}} + \frac{\partial \Phi}{\partial \sigma_M}\Big|_{\substack{\tau=\tau_0\\ q=q_0}} \dot{\sigma}_M + \frac{\partial \Phi}{\partial f}\Big|_{\substack{\tau=\tau_0\\ q=q_0}} \dot{f}. \tag{5.20}$$

Table 1. Numerical procedure of the solution of elastic-plastic problem.

A) geometrical update

1) $\mathbf{u}_{n+1} = \mathbf{u}_n + \Delta\mathbf{u}$

2) deformation gradient for the incremental objective integration

$\mathbf{F}_{n+\alpha} = \alpha\mathbf{F}_{n+1} + (1-\alpha)\mathbf{F}_n$

3) increment of strains

$\Delta\mathbf{E} = \mathbf{E}_{n+1} - \mathbf{E}_n$

B) elastic predictor

1) push forward of the stress and the back stress tensor

${}^{FL}\tau^{ij}_{n+1}$ from τ^{ij}_n; ${}^{FL}\alpha^{ij}_{n+1}$ from α^{ij}_n

2) elastic constitutive equation with the *Zaremba–Jaumann* derivative of the *Kirchhoff* stress tensor

$P^{ijkl} = C^{ijkl} - {}^{FL}\tau^{ik}_{n+1} g^{jl} - {}^{FL}\tau^{kj}_{n+1} g^{il}$

3) calculation of stress

${}^{(0)}\tau^{ij}_{n+1} = \tau^{ij}_n + P^{ijkl}\Delta E_{kl}$

4) calculation of the back stress tensor

${}^{(0)}\alpha^{ij}_{n+1} = \alpha^{ij}_n - ({}^{FL}\alpha^{ik}_{n+1} g^{jl} + {}^{FL}\alpha^{kj}_{n+1} g^{il})\Delta E_{kl}$

C) check the yield condition

${}^{(0)}\sigma_{M,n+1} = \sigma_{M,n}$; ${}^{(0)}f_{n+1} = f_n$

${}^{(0)}\Phi_{n+1} = \Phi({}^{(0)}\tau^{ij}_{n+1}, {}^{(0)}\alpha^{ij}_{n+1}, {}^{(0)}\sigma_{M,n+1}, {}^{(0)}f_{n+1}) \leq 0$?

yes: $\tau^{ij}_{n+1} = {}^{(0)}\tau^{ij}_{n+1}$; $\alpha^{ij}_{n+1} = {}^{(0)}\alpha^{ij}_{n+1}$; $\sigma_{M,n+1} = {}^{(0)}\sigma_{M,n+1}$; $f_{n+1} = {}^{(0)}f_{n+1}$

no: $i = 0$

D) plastic corrector

$\Delta\Lambda = \dot{\Lambda} \cdot \Delta t$ in accordance with Eqs. (5.21) and (5.22)

$${}^{(i+1)}\tau^{ij}_{n+1} = {}^{(i)}\tau^{ij}_{n+1} - \Delta\Lambda C^{ijkl} \frac{\partial \Phi}{\partial {}^{(i)}\tau^{kl}_{n+1}}$$

$${}^{(i+1)}\alpha^{ij}_{n+1} = {}^{(i)}\alpha^{ij}_{n+1} + R\,\Delta\Lambda({}^{(i)}\tau^{ij}_{n+1} - {}^{(i)}\alpha^{ij}_{n+1})$$

$${}^{(i+1)}\sigma_{M,n+1} = {}^{(i)}\sigma_{M,n+1} + \Delta\Lambda \frac{b^{\xi}}{{}^{(i)}\sigma_{M,n+1}(1-{}^{(i)}f_{n+1})} ({}^{(i)}\tau^{ij}_{n+1} - {}^{(i)}\alpha^{ij}_{n+1}) \frac{\partial \Phi}{\partial {}^{(i)}\tau^{ij}_{n+1}}$$

$${}^{(i+1)}f_{n+1} = {}^{(i)}f_{n+1} + \Delta\Lambda(1-{}^{(i)}f_{n+1}) \frac{\partial \Phi}{\partial {}^{(i)}\tau^{ii}_{n+1}}$$

E) convergence check

$\Phi({}^{(i+1)}\tau^{ij}_{n+1}, {}^{(i+1)}\alpha^{ij}_{n+1}, {}^{(i+1)}\sigma_{M,n+1}, {}^{(i+1)}f_{n+1}) \leq \varepsilon$?

yes: $\tau^{ij}_{n+1} = {}^{(i+1)}\tau^{ij}_{n+1}$; $\alpha^{ij}_{n+1} = {}^{(i+1)}\alpha^{ij}_{n+1}$; $\sigma_{M,n+1} = {}^{(i+1)}\sigma_{M,n+1}$; $f_{n+1} = {}^{(i+1)}f_{n+1}$

no: $i \leftarrow i+1$, go to D)

With the evolution equations, proposed in Sect. 4.2, it is possible to express all the increments in Eq. (5.20) in terms of $\dot{\Lambda}$. The *Newton–Raphson* algorithm is obtained when Eq. (5.20) is set to zero. $\dot{\Lambda}$ is calculated as

$$\dot{\Lambda} = \frac{\Phi|_{\substack{\tau=\tau_0 \\ q=q_0}}}{\Sigma}, \tag{5.21}$$

$$\Sigma = \left.\frac{\partial \Phi}{\partial \tau}\right|_{\substack{\tau=\tau_0 \\ q=q_0}} : \mathbf{C} : \frac{\partial \Phi}{\partial \boldsymbol{\tau}} + R \left.\frac{\partial \Phi}{\partial \tau}\right|_{\substack{\tau=\tau_0 \\ q=q_0}} : (\boldsymbol{\tau} - \boldsymbol{\alpha}) - \left.\frac{\partial \Phi}{\partial \sigma_M}\right|_{\substack{\tau=\tau_0 \\ q=q_0}} \frac{b\xi}{(1-f)\sigma_M} \frac{\partial \Phi}{\partial \boldsymbol{\tau}} : (\boldsymbol{\tau} - \boldsymbol{\alpha}) - \left.\frac{\partial \Phi}{\partial f}\right|_{\substack{\tau=\tau_0 \\ q=q_0}} (1-f)\,\mathrm{tr}\,\frac{\partial \Phi}{\partial \boldsymbol{\tau}}. \tag{5.22}$$

A more detailed description of the procedure is listed in Table 1. Geometrically, the calculation can be interpreted as the projection of the point in the stress space, obtained by the elastic predictor step, onto a sequence of linearized yield surfaces. The iteration is terminated when the yield condition is satisfied within a given tolerance.

6. Examples

The finite element formulations pointed out are implemented in the general purpose computer program FEAP, developed by R. L. TAYLOR and described in ZIENKIEWICZ [14].

Two examples will be considered to illustrate the correctness of formulation and to describe the constitutive behaviour of the material: the problem of simple shear and the necking of a cylindrical bar.

6.1. The problem of simple shear

The problem of simple shear is used to verify the computational results in case of *Mises* material with combined isotropic-kinematic hardening without voids. The finite

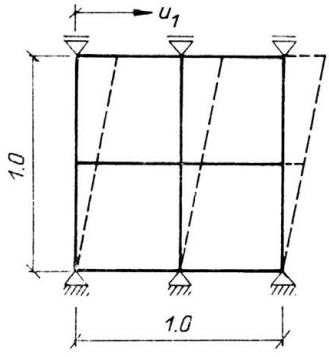

FIG. 1. Discretized model of simple shear.

element mesh is shown in Fig. 1. The shear deformation is enforced by a displacement rate, subjected to the nodes at the top of the structure.

Consider a material with purely kinematic hardening and with application of the *Zaremba–Jaumann* derivative in the evolution equation of the back-stress tensor $\boldsymbol{\alpha}$. A semi-analytical solution is presented by ATLURI [52] for the ratio $\sigma_y/G = 0.1225$, where σ_y denotes the yield stress and G the elastic shear modulus. The ensuing stress-displacement relation and the components of the back stress tensor as a function of the displacements are displayed in Figs. 2 and 3, respectively.

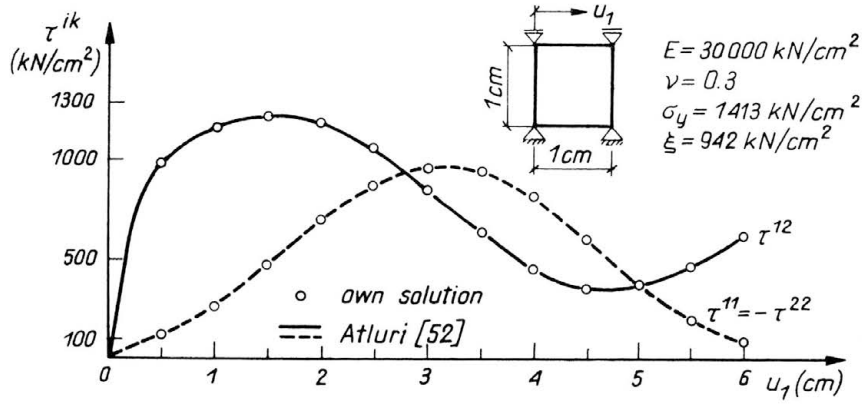

FIG. 2. Simple shear, kinematic hardening with application of the Zaremba–Jaumann rate. Comparison of the computed stress-strain relation with the solution of ATLURI [52].

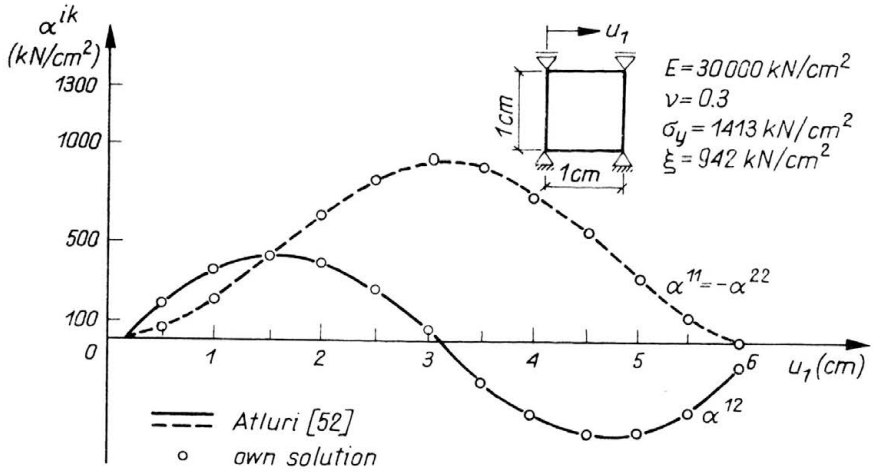

FIG. 3.Simple shear, kinematic hardening with application of the Zaremba–Jaumann rate. Comparison of the computed back stress-strain relations with the solution of ATLURI [52].

From there it can be seen that the computational results agree with the semi-analytical solution. This illustrates the correct implementation of the equations describing phenomena in the finite deformation range. On the other hand, the well-known oscilla-

tory behavior of the components of the stress tensor and the back stress tensor can be observed.

In a physical sense, more realistic results are obtained when the time derivative proposed by PAULUN, PĘCHERSKI [11] is applied in the evolution equation of the back stress tensor. In order to have a small influence of elastic material behavior, which is neglected in [11], a small initial yield stress and a large *Young* modulus were chosen. The material constants were taken from an aluminium alloy: $\sigma_y = 207$ MPa, and $\xi = 414$ MPa. The solution given in [11] as well as the numerical results are displayed in Fig. 4.

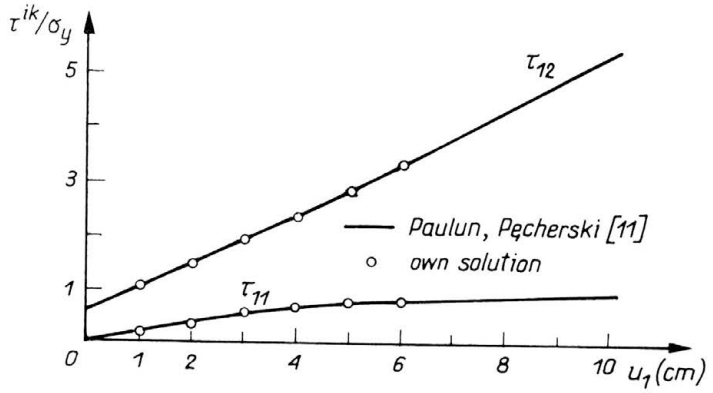

FIG. 4. Simple shear, kinematic hardening with the application of the substructure corotational rate (cf. PAULUN and PĘCHERSKI [11]). Comparison of the computed stress-strain relation with the solution obtained in [11].

It is visible that the shear stress and the normal stress increase now monotonously with the displacement. Again, there is a good agreement between the finite element solution and the semi-analytical results.

6.2. Necking of a circular cylindrical bar

Consider a circular cylindrical bar in uniaxial tension enforced by an axial displacement rate at the ends of the bar. The geometric data and the finite element discretization are given in Fig. 5. The material properties are: $E = 210{,}000$ MPa, $v = 0.3$, $\sigma_y = 200$ MPa. The hardening function of the material is given by the modified *Ramberg-Osgood* law

$$\varepsilon^p = \frac{1.1\sigma_y}{mE}\left[\left(\frac{\sigma_e}{1.1\sigma_y}\right)^m - \left(\frac{1}{1.1}\right)^m\right], \tag{6.1}$$

which has been used, e.g., by ARGYRIS, DOLTSINIS, KLEIBER [53] and KLEIBER [54]. The hardening exponent is assumed to be 8. The ends of the bar are cemented to rigid grips. A small geometric imperfection has been given to the model prior to loading.

Various calculations with different constitutive assumptions are carried out:
isotropic hardening and kinematic hardening without voids,

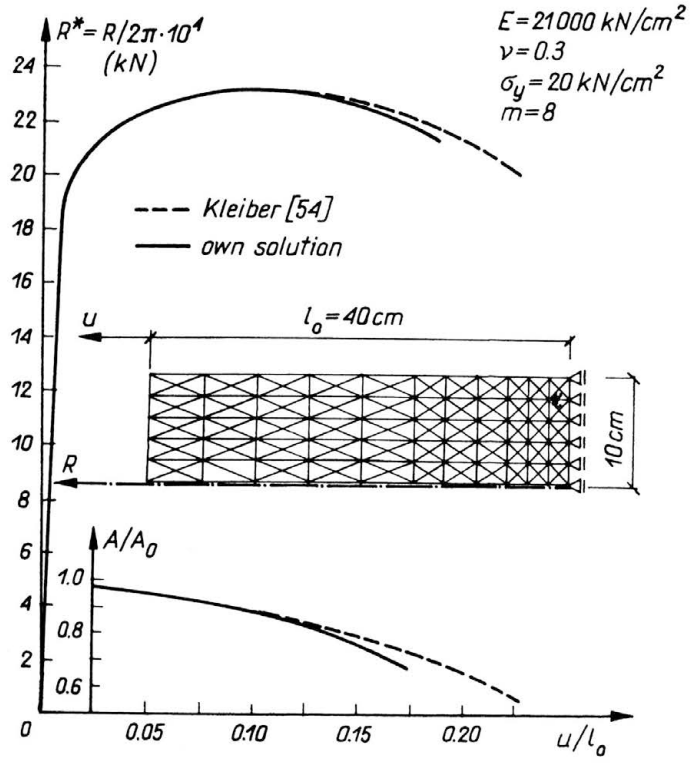

FIG. 5. Necking of a circular cylindrical bar for isotropic hardening without voids. Load–displacement diagram and the diagram displaying the reduction of the midcross-section with increasing axial elongation. Comparison with the computational results obtained by KLEIBER [54].

isotropic hardening and kinematic hardening with an initial void volume fraction $f = 0.04$.

In case of isotropic hardening without voids, the results can directly be compared with those of KLEIBER [54]. In Fig. 5 both solutions are presented in the load-displacement diagram as well as in the diagram, displaying the reduction of the midcross section with increasing axial elongation.

There is a good agreement between the curves up to the maximum of load. However, in the present study the maximum is reached at an axial elongation $u/l_0 = 0.053$, whereas in Kleiber's solution it is calculated at $u/l_0 = 0.06$. This difference may result from the finite element discretization which is finer in the necking region in the present study.

In Fig. 6 the same results are presented, but now kinematic hardening takes place. It is visible that the results do not differ from those calculated with isotropic hardening up to the maximum of the load deflection curve. In the case of kinematic hardening, however, the maximum is reached at an axial elongation $u/l_0 = 0.051$ which is a little less than in the case of isotropic hardening. Furthermore, the curve applied to kinematic hardening decreases much more with further elongation. The deformed mesh at maximum load is shown in Fig. 7.

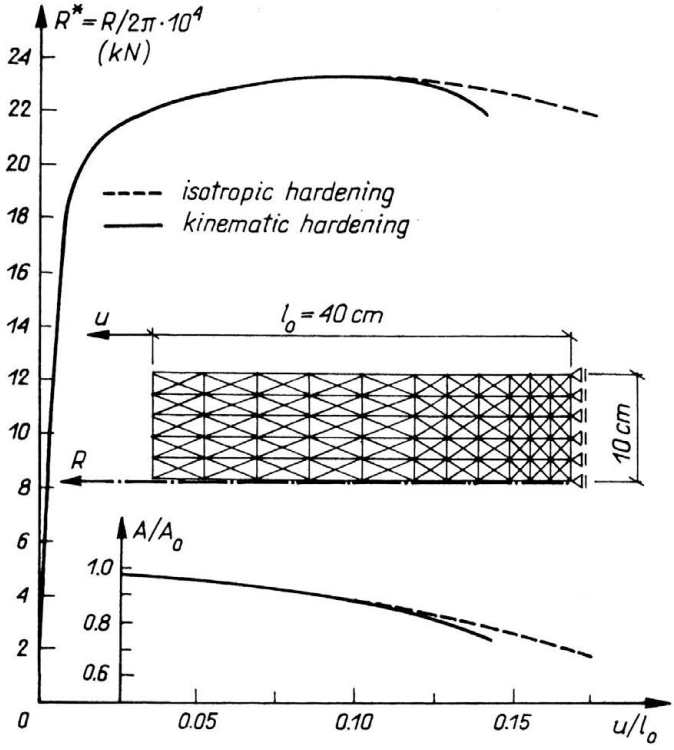

FIG. 6. Necking of a circular cylindrical bar for isotropic and kinematic hardening without voids. Effect of kinematic hardening on the load-displacement and the reduction of the midcross section with increasing axial elongation.

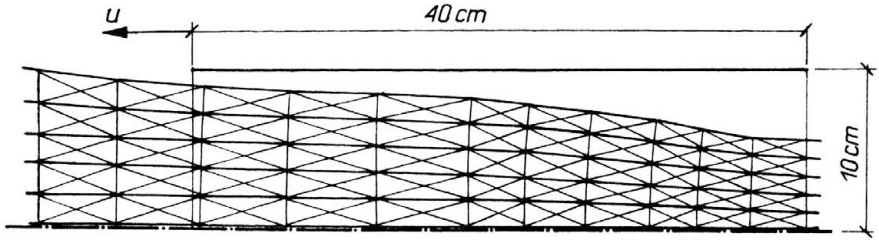

Fig. 7. Necking of a circular cylindrical bar. The deformed mesh at maximum load.

These results agree with the studies of different authors (e.g., MEAR, HUTCHINSON [8], TVERGAARD [9])., acknowledging that the increasing yield surface curvature favours plastic localization.

In case of materials with voids the results are displayed in Figs. 8 and 9. In the load-displacement diagram all the curves coincide up to the maximum load. Those referred to the void containing material, however, descend steeper than the corresponding ones, referring to voidless material, Fig. 8. Furthermore, it is visible in Fig. 9, that the void

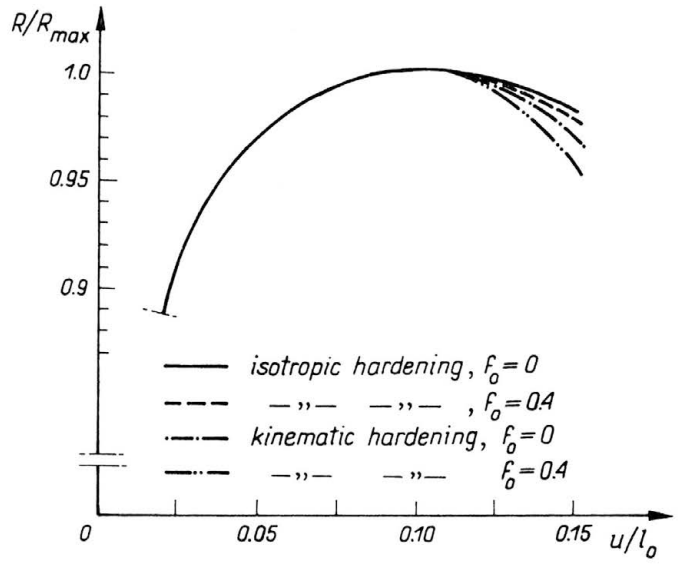

FIG. 8. Necking of a circular cylindrical bar for isotropic and kinematic hardening. Comparison of the load — elongation diagrams for the voidless material with the material with the initial void volume fraction $f = 0.4$.

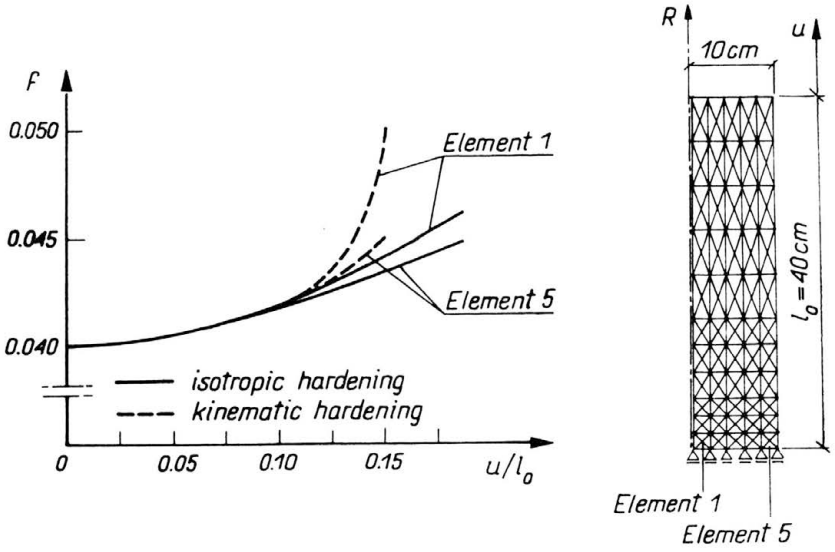

FIG. 9. Necking of a circular cylindrical bar for isotropic and kinematic hardening. The effect of kinematic hardening on the development of voids in the different parts of the midcross-section.

volume fraction increases much faster in case of kinematic hardening. So it can be seen again that kinematic hardening favours plastic localization. Just like in experiments, the greatest amount of the void volume fraction takes place in the center of the bar.

Appendix

In this appendix a brief summary of the notation and basic concepts of differential geometry employed in this paper is given. The work of tensor analysis on manifolds of ABRAHAM, MARSDEN and RATIU [55] as well as the texts on the applications for the continuum mechanics of MARSDEN and HUGHES [33] may be consulted for further details.

Consider smooth orientable *Riemannian* manifolds $(B, \mathbf{G})$ and $(S, \mathbf{g})$ endowed with *Riemannian* metrics $\mathbf{G}$ and $\mathbf{g}$, respectively. B can be understood as the fixed reference configuration of the body and S is the ambient space in which the motion of the body takes place. Denoting by $C := \{\varphi: B \to S | \varphi \text{ is } C^\infty \text{ embedding}\}$ the configuration space, a motion of the body is the curve of configurations $t \in \mathbf{R} \to \varphi_t(X) \in C$ and we can write

$$\mathbf{x} = \varphi_t(\mathbf{X}) = \varphi(\mathbf{X}, t), \quad \mathbf{X} \in B. \tag{A.1}$$

The motion φ_t determines the material velocity as a vector field over φ_t, i.e., $\mathbf{V}_t: B \to T_X S$, defined as

$$\mathbf{V}_t(\mathbf{X}) = \frac{\partial \varphi_t(\mathbf{X})}{\partial t}, \quad \mathbf{X} \in B \tag{A.2}$$

and the material acceleration $\mathbf{A}_t: B \to T_X S$,

$$\mathbf{A}_t(\mathbf{X}) = \frac{\partial \mathbf{V}_t(\mathbf{X})}{\partial t}, \quad \mathbf{X} \in B, \tag{A.3}$$

where $T_x S$ is the tangent space to S at $\mathbf{x}$.

The spatial velocity $\mathbf{v}_t: \varphi_t(B) \to T_{\varphi(X)} S$ and spatial acceleration $\mathbf{a}_t: \varphi_t(B) \to T_{\varphi(X)} S$ are defined as $\mathbf{v}_t = \mathbf{V}_t \circ \varphi^{-1}$ and $\mathbf{a}_t = \mathbf{A}_t \circ \varphi_t^{-1}$.

The *deformation gradient* $\mathbf{F}$ of φ is the tangent of φ; thus $\mathbf{F} = T\varphi$. For $\mathbf{X} \in B$, $\mathbf{F}(\mathbf{X})$ denote the restriction of $\mathbf{F}$ to $T_X B$. Thus $\mathbf{F}(\mathbf{X}): T_X B \to T_{\varphi(X)} S$ is a linear transformation for each $\mathbf{X} \in B$. If $\{x^i\}$ and $\{X^j\}$ denote coordinate systems on S and B, respectively, then the matrix of $\mathbf{F}(\mathbf{X})$ with respect to the coordinate bases $\mathbf{g}_i(\mathbf{x})$ and $\mathbf{G}_j(\mathbf{X})$, where $\mathbf{x} = \varphi(\mathbf{X})$, is given by

$$F^i_j(\mathbf{X}) = \frac{\partial \varphi^i(\mathbf{X})}{\partial X^j}. \tag{A.4}$$

If $\mathbf{t}$ is a tensor field, defined on the deformed configuration $\varphi_t(B)$, the *pull-back* of $\mathbf{t}$ through the motion φ_t defines a tensor field $\mathbf{T}$ on B denoted by $\mathbf{T} = \varphi_t^*(\mathbf{t})$. For example, in the case of a second order contravariant tensor the pull back operation takes the form

$$T^{jl} = (F^{-1})^j{}_i (F^{-1})^l{}_k (t^{ik} \circ \varphi_t), \tag{A.5}$$

or, in the absolute notation,

$$\mathbf{T} = \mathbf{F}^{-1} \cdot \mathbf{t} \cdot \mathbf{F}^{-T}. \tag{A.6}$$

Likewise, if $\mathbf{T}$ is a material tensor field defined on B, the *push-forward* of $\mathbf{T}$ through the motion φ_t defines a spatial tensor field $\mathbf{t}$ on $\varphi_t(B)$ denoted by $\mathbf{t} = \varphi_{t*}(\mathbf{T})$. In this case, for the example used above, the push-forward operation takes the form

$$t^{jl} = F^i{}_J F^k{}_l (T^{jl} \circ \varphi_t^{-1}), \tag{A.7}$$

or in the absolute notation

$$\mathbf{t} = \mathbf{F} \cdot \mathbf{T} \cdot \mathbf{F}^T. \tag{A.8}$$

Let $\mathbf{v}_t$ be the spatial velocity vector field of a motion φ_t. Then the collection $\{\varphi_{t,s} | \varphi_{t,s} = \varphi_t \circ \varphi_s^{-1} : \varphi_s(B) \to \varphi_t(B)\}$ is the *flow* or evolution operator of $\mathbf{v}_t$.

Definifion of the Lie derivative

Let $\mathbf{v}$ be a C^1 (time dependent) vector field on S and let $\varphi_{t,s}$ denote its flow. If $\mathbf{t}_t$ is a C^1 (possibly time-dependent) tensor field on S, the *Lie derivative* of $\mathbf{t}$ with respect to $\mathbf{v}$ is defined by

$$L_v \mathbf{t} = \left(\frac{d}{dt} \varphi_{t,s}^*(\mathbf{t}_t) \right) \Big|_{t=s} \equiv \varphi_{t*} \left(\frac{\partial}{\partial t} \varphi_t^*(\mathbf{t}_t) \right). \tag{A.9}$$

A general coordinate expression can be given for the Lie derivative of a tensor for arbitrary type, namely,

$$\begin{aligned} (L_v t)^{ab\ldots c}_{de\ldots f} &= \dot{t}^{ab\ldots c}_{de\ldots f} \\ &\quad - t^{gb\ldots c}_{de\ldots f} \frac{\partial v^a}{\partial x^g} - \text{all upper indices} \\ &\quad + t^{ab\ldots c}_{ke\ldots f} \frac{\partial v^k}{\partial x^d} + \text{all lower indices}, \end{aligned} \tag{A.10}$$

where

$$\dot{t}^{ab\ldots c}_{de\ldots f} = \frac{\partial}{\partial t} t^{ab\ldots c}_{de\ldots f} + \frac{\partial}{\partial x^g} t^{ab\ldots c}_{de\ldots f} v^g. \tag{A.11}$$

It is essential to note that such operations as pull-back and push-forward as well as the Lie derivative have no unique representations, i.e., they do not commute with lowering and raising of indices. The sufficient and necessary condition that these representations are unique is that $\mathbf{v}$ be a *Killing vector field* for the *Riemannian* metric $\mathbf{g}$.

When a map $\Psi : S \to S$ is an isometry of a metric $\mathbf{g}$, i.e., $\Psi^* \mathbf{g} = \mathbf{g}$, a vector field $\mathbf{v}$ is a *Killing vector field* (or infinitesimal isometry) if each map $\Psi_{t,s}$ of the flow of $\mathbf{v}$ is an isometry in S.

Aknowledgements

This paper has been prepared during the visits of R.B.P. to the Institut für Baumechanik und Numerische Mechanik, Universität Hannover, as a fellow of the Alexander von Humboldt Foundation and R. L. to the Institute of Fundamental Technological Research, Polish Academy of Sciences (PAS), in Warsaw within the framework of the exchange program between the Deutsche Akademische Austauschdienst and PAS. The financial support of the institutions mentioned is gratefully acknowledged.

References

1. T. J. R. HUGHES, *Numerical implementation of constitutive models: rate-independent deviatoric plasticity* in: Proc. the Workshop on the Theoretical Foundation for Large-Scale Computations of Nonlinear Material Behavior, Evanston, Illinois, October 24, 25 and 26, 1983, S. NEMAT-NASSER *et al.* [eds.], Martinius Nijhoff Publishers, Dordrecht, Boston, Lancaster, pp. 29–63, 1984.
2. A. L. GURSON, *Plastic flow and fracture behavior of ductile materials incorporating void nucleation, growth and interaction*, Ph. D. Thesis, Division of Engineering, Brown University, Providence, R. I., 1975.
3. A. L. GURSON, *Continuum theory of ductile rupture by void nucleation and growth — I. Yield criteria and flow rules for porous ductile media*, J. Eng. Mat. Tech., **99**, 2–15, 1977.
4. A. NEEDLEMAN and J. R. RICE, *Limits to ductility set by plastic flow localization*, in: Mechanics of Sheet Metal Forming, D. P. KOISTINEN *et al.* [eds.], Plenum Publishing Corporation, 237–267, 1978.
5. V. TVERGAARD, *Material failure by void growth to coalescence*, The Technical University of Denmark, Report No. S 45, July 1988 [to appear in Adv. in Appl. Mech.]
6. V, TVERGAARD, *Effect of kinematic hardening on localized necking in biaxially streched sheets*, Int. J. Mech. Sci., **20**, 651–658, 1978.
7. J. W. HUTCHINSON and V. TVERGAARD, *Shear band formation in plain strain*, Int. J. Solids and Structures, **17**, 451–470, 1981.
8. M. E. MEAR and J. W. HUTCHINSON, *Influence of yield surface curvature on flow localization in dilatant plasticity*, Mech. Mat., 4, 395–407, 1985.
9. V. TVERGAARD, *Effect of yield surface curvature and void nucleation on plastic flow localization*, J. Mech. Phys. of Solids, **35**, 43–60, 1987.
10. M. DUSZEK and P. PERZYNA, *Plasticity of damaged solids and shear band localization*, Ingenieur Archiv, **58**, 380–392, 1988.
11. J. E. PAULUN and R. B. PĘCHERSKI, *Study on corotational rates for kinematic hardening in finite deformation plasticity*, Arch. Mech., **37**, 661–677, 1985.
12. J. E. PAULUN and R. B. PĘCHERSKI, *On the application of the plastic spin concept for the description of anisotropic hardening in finite deformation plasticity*, Int. J. Plasticity, 3, 303–314, 1987.
13. R. B. PĘCHERSKI, *The plastic spin concept and the theory of finite plastic deformations with induced anisotropy*, Arch. Mech., **40**, 807–818, 1988.
14. O. C. ZIENKIEWICZ, *The finite element method*, McGraw Hill, London, 3rd ed., 1977.
15. A. NEEDLEMAN and V. TVERGAARD, *Finite element analysis of localization plasticity*, in: Finite Elements, Vol. V, Special Problems in Solid Mechanics, J. T., ODEN and G. F. CAREY, [eds.], Prentice-Hall, Englewood Cliffs, pp 94–157, 1984.
16. M. KLEIBER, *Incremental finite element modelling in non-linear solid mechanics*, PWN-Polish Scientific Publishers, Warszawa and Ellis Horwoord Ltd., Chichester 1989.
17. T. K. HELLEN, *A numerical evaluation of elastic-plastic algorithms*, in: Proc. 2nd International Conference on Computational Plasticity, Models, Software and Applications, Vol I, Barcelona, September 18–22, 1989, D. R. J. OWEN *et al.* [eds.], Pineridge Press, Swansea, pp 359–375, 1989.
18. P. M. PINSKY, M. ORTIZ and R. T. TAYLOR, *Operator split methods in the numerical solution of the finite deformation elastoplastic dynamic problem*, Comp. and Struct., 17, 345–359, 1983.
19. M. L. WILKINS, *Calculation of elastic-plastic flow*, Meth. Comp. Phys., Vol. 3, B. ALDER, *et al.* [eds.], Academic Press, 1964.
20. R. D. KRIEG and D. B. KRIEG, *Accuracies of numerical solution methods for the elastic-perfectly plastic model*, ASME, J. Press, Vess. Tech., **99**, 510–515, 1977.
21. H. L. SCHREYER, R. F. KULAK and M. M. KRAMER, *Accurate numerical solutions for elastic-plastic models*, ASME, J. Press. Vess. Tech., **101**, 226–234, 1979.
22. R. D. KRIEG and S. W. KEY, *Implementation of a time-dependent plasticity theory into structural computer programs*, in: Constitutive Equations in Viscoplasticity: *Computational and Engineering Aspects*, J. A. STRICKLIN and K. J. SACZALSKI [eds.], AMD-20, ASME, New York, 1976.
23. M. ORTIZ, *Topics in constitutive theory for inelastic solids*, Ph. D. Thesis, Dept. of Civil Engineering, University of California, Berkeley, CA 1981.

24. M. ORTIZ, P. M. PINSKY and R. L. TAYLOR, *Operator split methods for the numerical solution of the elastoplastic dynamic problem*, Comp. Meth. Appl. Mech. Eng., **39**, 137–157, 1983.
25. L. PLANK and E. STEIN, *Projektionsverfahren zur iterativen Berechnung elastoplastischer Deformationen*, Techn. Rep. No. S85/3, Inst. für Baumechanik, Universität Hannover, 1985.
26. M. ORTIZ and J. C. SIMO, *An analysis of a new class of integration algorithms for elastoplastic constitutive relations*, Int. J. Num. Meth. Eng., **23**, 353–366, 1986.
27. J. C. SIMO and M. ORTIZ, *A unified approach to finite deformation elastoplastic analysis on the use of hyperelastic constitutive equations*, Comp. Meth. Appl. Mech. Eng., **49**, 221–245, 1985.
28. J. C. SIMO and R. L. TAYLOR, *Consistent tangent operators for rate-independent elastoplasticity*, Comp. Meth. Appl. Mech. Eng., **48**, 101–118, 1985.
29. J. C. NAGTEGAAL, *On the implementation of inelastic constitutive equations with special reference to large deformation problems*, Comp. Meth. Appl. Mech. Eng., **33**, 469–484, 1982.
30. T. J. R. HUGHES and K. S. PISTER, *Consistent linearization in mechanics of solids and structures*, Comp. and Struct., **8**, 391–397, 1978.
31. P. WRIGGERS, *Konsistente Linearisierungen in der Kontinuumsmechanik und ihre Anwendung auf die Finite Element Methode*, Techn. Rep. No. F88/4, Inst. für Baumechanik, Universität Hannover, 1988.
32. F. GRUTTMANN and E. STEIN, *Tangentiale Steifigkeitsmatrizen bei Anwendung von Projektionsverfahren in der Elastoplastizitätstheorie*, Ing. Archiv, **58**, 15–24, 1988.
33. J. E. MARSDEN and T. J. R. HUHGES, *Mathematical foundations of elasticity*, Prentice Hall, Englewood Cliffs, NJ, 1983.
34. J. C. SIMO, *A framework for finite strain elastoplasticity based on maximum plastic dissipation and on the multiplicative decomposition. Part I. Continuum formulation*, Comp. Meth. Appl. Mech. Eng., **66**, 199–219, 1988.
35. P. PERZYNA, *Constitutive equations of dynamic plasticity*, in: Engineering Application of Modern Plasticity, Proc. of Post Symposium Short Course of the 2nd International Symposium of Plasticity, Nagoya, August 4–5, 1989, pp. 1–18.
36. GUO ZHONG-HENG, *Time derivatives of tensor fields in non-linear continuum mechanics*, Arch. Mech., **15**, 131–163, 1963.
37. A. E. GREEN and W. ZERNA, *Theoretical plasticity*, Oxford University Press, Oxford 1968.
38. A. NEEDLEMAN, *Finite elements for finite strain plasticity problems*, in: Proc. Workshop on Plasticity of Metals at Finite Strain: Theory, Experiment and Computation, Stanford University, 1981, E. H. LEE and R. L. MALLET [eds.], published by the Div. Appl. Mech., Stanford University and Dept. of Mech. Eng. Aeronautical Eng. and Mechanics, R. P. I. Troy, 1982.
39. P. M. PINSKY, M. ORTIZ and K. S. PISTER, *Numerical integration of rate constitutive equations in finite deformation analysis*, Comp. Meth. Appl. Mech. Eng., **40**, 137–158, 1983.
40. R. LAMMERING, *Beiträge zur Theorie und Numerik grosser plastischer und kleiner elastischer Deformationen mit Schädigungseinfluss*, Ph. D. Dissertation, Techn. Rep. No. F88/3, Inst. für Baumechanik, Universität Hannover, 1988.
41. M. KLEIBER and B. RANIECKI, *Elastic-plastic materials at finite strains*, in: Plasticity today, Modelling, Methods and Applications, A. SAWCZUK and G. BIANCHI [eds.], Proc. Int. Symposium on Current Trends and Results in Plasticity, CISM, Udine, Italy, June 1983, Elsevier, London-New York 3–46, 1985.
42. J. MANDEL, *Plasticité classique et viscoplasticité*, Courses and Lectures, CISM, Udine, Springer, New-York 1971.
43. B. LORET, *On the effects of plastic rotation in the finite deformation of anisotropic elastoplastic materials*, Mech. Materials, 2, 287–304, 1983.
44. F. SIDOROFF and C. TEODOSIU, *Microstructure and phenomenological models for metals*, in: Large Deformations of Solids: Physical Basis and Mathematical Modelling, J. GITTUS et al. [eds.], Elsvier, London, New York, p. 163, 1986.
45. Y. E. DAFALIAS, *Issues on the constitutive formulation at large elastoplastic deformations, Part I. Kinematics*, Acta Mech., **69**, 119–138, 1987.

46. B. RANIECKI and S. K. SAMANTA, *The thermodynamic model of a rigid-plastic solid with kinematic hardening, plastic spin and orientation variables*, Arch. Mech., **41**, 4, 1989.
47. P. WRIGGERS and E. STEIN, *Die Verwendung von Lie-Ableitungen bei der Angabe von Spannungsflüssen für große Deformationen*, Z. Angew. Math. Mech., **68**, T264–T267, 1988.
48. W. PRAGER, *An elementary discussion of definitions of stress rate*, Quart. Appl. Math., 18, 403–407, 1961.
49. B. RANIECKI and H. V. NGUYEN, *Isotropic elastic-plastic solids at finite strain and arbitrary pressure*, Arch. Mech., **36**, 687–704, 1984.
50. J. F. W. BISHOP and R. HILL, *A theory of the plastic distortion of a polycristalline aggregate under combined stresses*, Phil. Mag., 42, 414–427, 1951.
51. C. A. BERG, *Plastic dilation and void interaction*, in: Inelastic Bahavior of Solids, M. F. KANNINEN *et al.* [eds.], McGraw-Hill, 171–207, 1970.
52. S. N. ATLURI, *On constitutive relations at finite strain. Hypo-elasticity and elasto-plasticity with isotropic or kinematic hardening*, Comp. Meth. Appl. Mech. Eng., **43**, 137–171, 1984.
53. J. H. ARGYRIS, J. St. DOLTSINIS and M. KLEIBER, *Incremental formulation in nonlinear mechanics and large strain elasto-platicity, Natural approach, Part I and II*, Comp. Meth. Appl. Mech. Eng., **11**, 215–247, 1977; **14**, 259–294, 1978.
54. M. KLEIBER, *On plastic localization and failure in plane strain and round voids containing tensile bars*, Int. J. Plasticity, 2, 205–221, 1986.
55. R. ABRAHAM, J. E. MARSDEN and T. RATIU, *Manifolds, tensor analysis and applications*, Springer, New York, 1988.

INSTITUT FÜR AEROELASTIK
DEUTSCHE FORSCHUNSANSTALT FÜR LUFT- UND RAUMFART, GÖTTINGEN,
POLISH ACADEMY OF SCINCES
INSTITUTE OF FUNDAMENTAL TECHNOLOGICAL RESEARCH
and
INSTITUT FÜR BAUMECHANIK UND NUMERISCHE MECHANIK
UNIVERSITÄT HANNOVER, GERMANY.

Received December 14, 1989.